2.0 AREA OF REVIEW AND CORRECTIVE ACTION PLAN
40 CFR 146.84(b)

MARQUIS BIOCARBON PROJECT

Facility Information

Facility name: MARQUIS BIOCARBON PROJECT

Facility contact: ELIZABETH STEINHOUR
DIRECTOR OF ENVIRONMENTAL AFFAIRS
10000 MARQUIS DRIVE, HENNEPIN, IL 61327
815.925.7300 / BETHSTEINHOUR@MARQUISENERGY.COM

Well name: MCI CCS 3
Well location: PUTNAM COUNTY, ILLINOIS
S2 T32N R2W
Latitude: 41.27026520 N, Longitude: 89.30939322 W

Table of Contents

List of Tables

List of Figures

2.0 <u>AoR and Corrective Action Plan</u>

2.1 Computational Modeling Approach

2.1.1   Model Background

Computational modeling at the Marquis BioCarbon Project site was completed to delineate the plume size and shape, area of pressure buildup, and Area of Review (AoR) for injected carbon dioxide (CO_2). A static earth model (SEM) named Marquis_SEM_1 was prepared by Battelle using the Schlumberger Petrel® modeling software. The SEM is a three-dimensional (3D) geocellular model that represents petrophysical properties within the stratigraphic formation intended for CO_2 storage, as well as the overlying confining layer. This type of model offers the best options for quantifying, visualizing, and simulating dynamic behavior through the subsurface geology at the site. By integrating multiple data types, the model represents the spatial distribution of available pore space and flow potential (permeability), enabling a data-driven estimation of CO_2 storage capacity. The SEM serves as the framework (in terms of delineating zones, surfaces, porosity, and permeability) for dynamic simulation of CO_2 injection.

Computational modeling to simulate CO_2 injection into the saline aquifer was completed by Battelle using the 3D multiphase flow simulator CMG-GEM version 2016 (CMG-GEM, 2016). In addition to the geological framework and associated properties imported from the SEM, parameters such as relative permeability, initial reservoir conditions, phase behavior, and well completion were added to the dynamic model for simulation. CMG-GEM is an equation-of-state based compositional simulator that models the phase behavior of brine and CO_2 plumes during the injection and post-injection stages of a project.

Aqueous, gaseous, and supercritical phases of CO_2 were accounted for in the computational model. Component transport equations, which describe the thermodynamic equilibrium between gaseous or supercritical with aqueous phases, were used in the compositional simulator to model CO_2 injection into the saline aquifer (Nghiem et al., 2004). The Peng-Robinson equation of state was used to model the fluid properties of the injected CO_2 in gaseous/supercritical phases (Peng and Robinson, 1976). The solubility of the injected CO_2 in brine is modeled as a phase equilibrium process, which is computed using Henry's law to estimate the fugacity of the gaseous and aqueous phases as functions of pressure and temperature (Li and Nghiem, 1986; Enick and Klara, 1990; Nghiem et al., 2009a). Additionally, the viscosity and density of the aqueous phase were calculated as functions of pressure, temperature, and salinity. Rowe and Chow (1970) equation was used to estimate aqueous phase density, and the Kestin et al. (1981) correlation was used to estimate the viscosity of the aqueous fluids.

2.1.2   Site Geology and Hydrology

The subsurface geologic and hydrologic data analyzed in this study were acquired from the nearby characterization well, MCI MW 1, drilled in 2021. The characterization data types, and depth coverages are detailed in the Pre-Operational Testing Program (Permit Section 5). Publicly available geologic and hydrologic data in the region, as well as well data, were compiled from well databases held by the Illinois State Geological Survey (ISGS).

Sensitive, Confidential, or Privileged Information
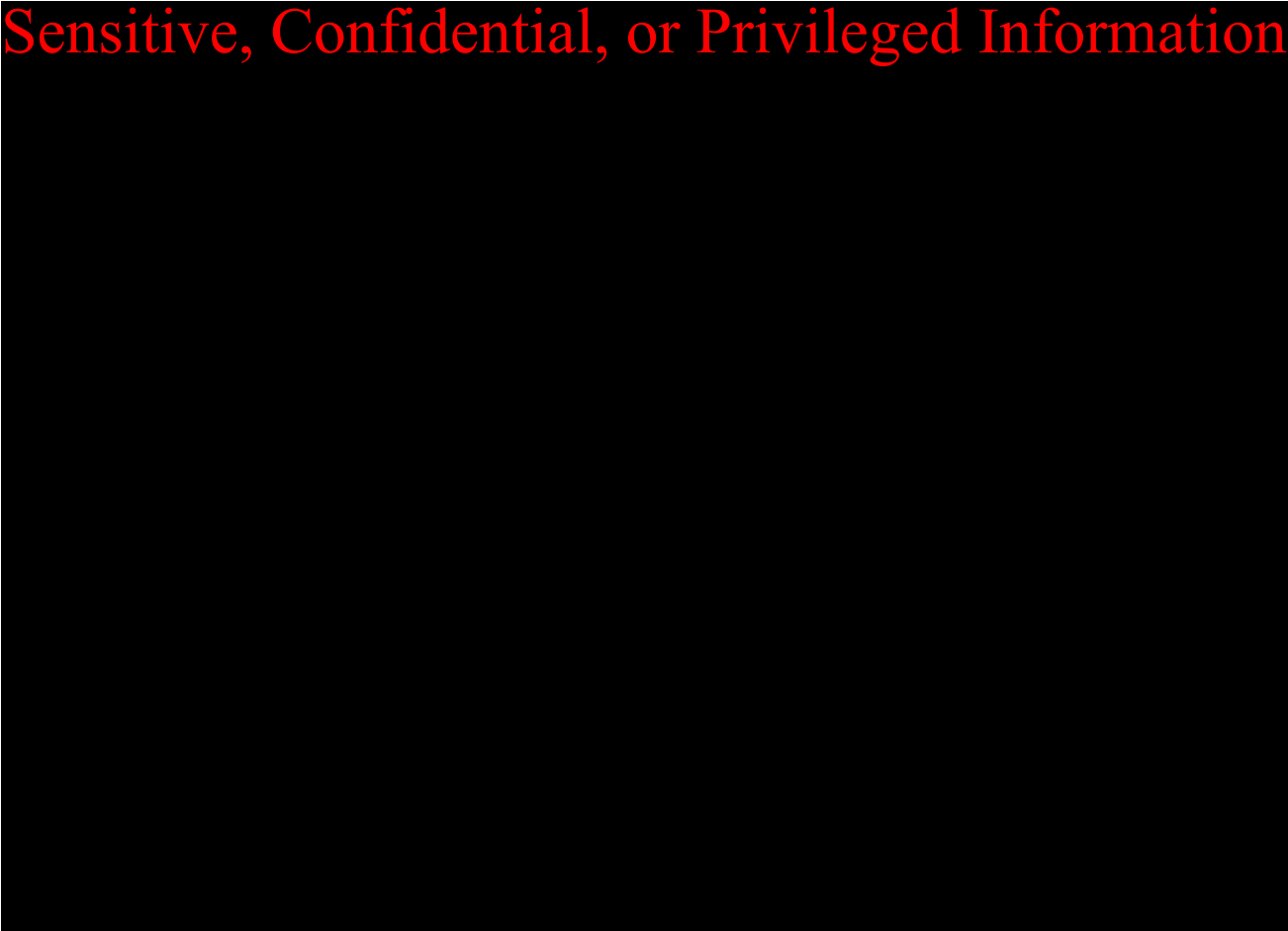
Sensitive, Confidential, or Privileged Information
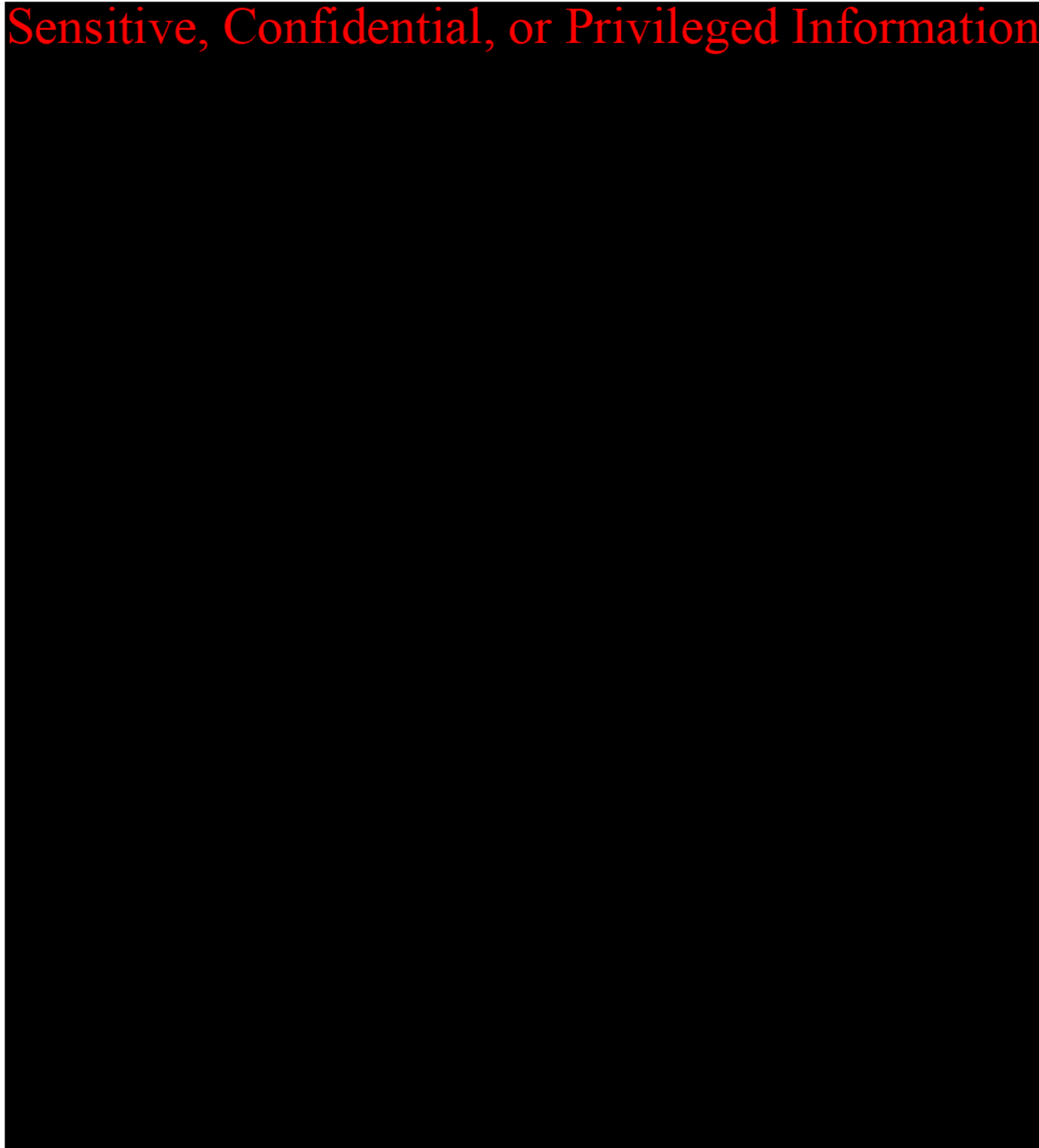
Figure 2-1: Stratigraphic column with lithology and hydrostratigraphy for the Marquis BioCarbon Project site based on data from the characterization well, MCI MW 1.

Sensitive, Confidential, or Privileged Information
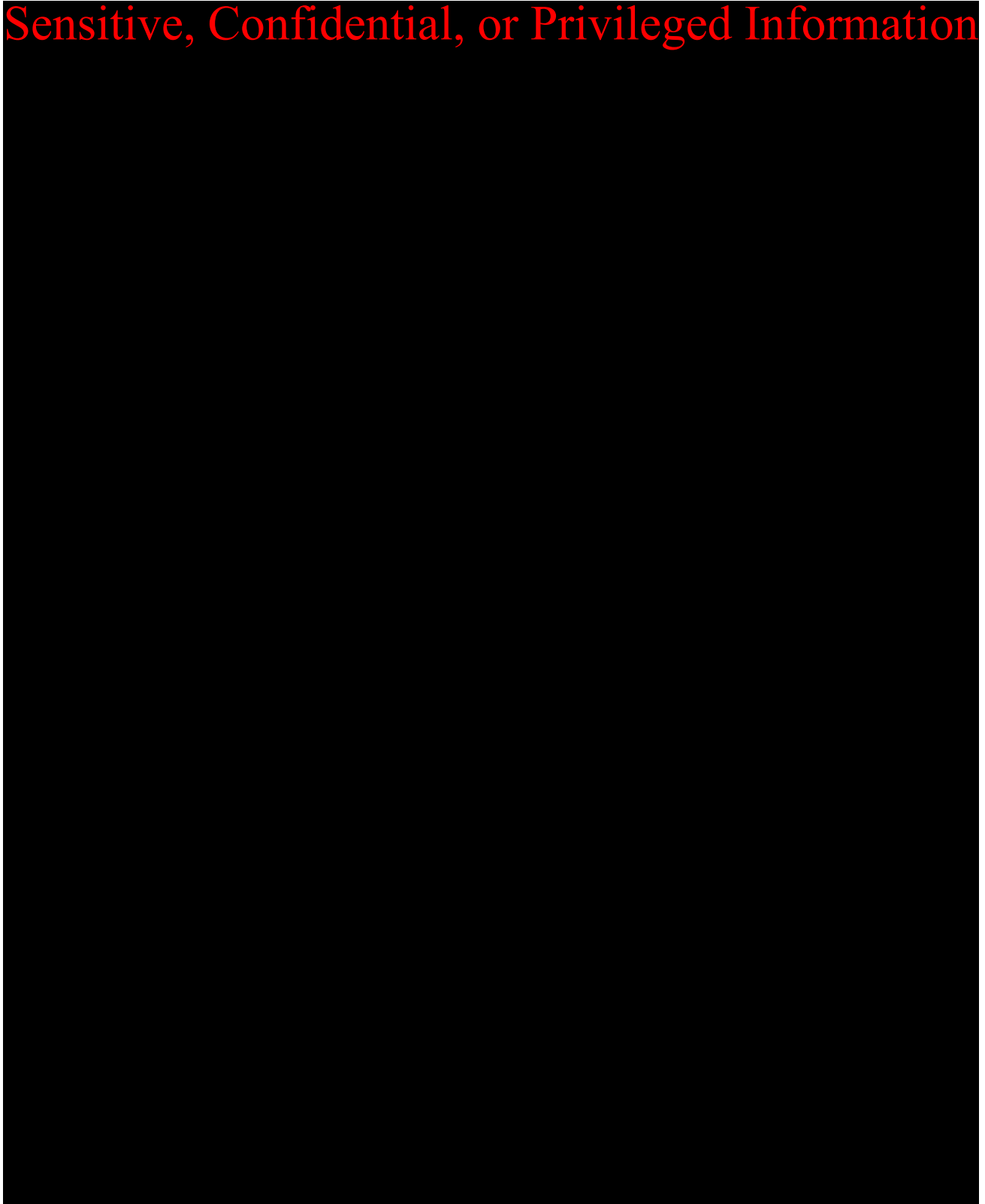
Figure 2-2: Precambrian basement elevation map. Modified from Willman et al. (1975).

Sensitive, Confidential, or Privileged Information
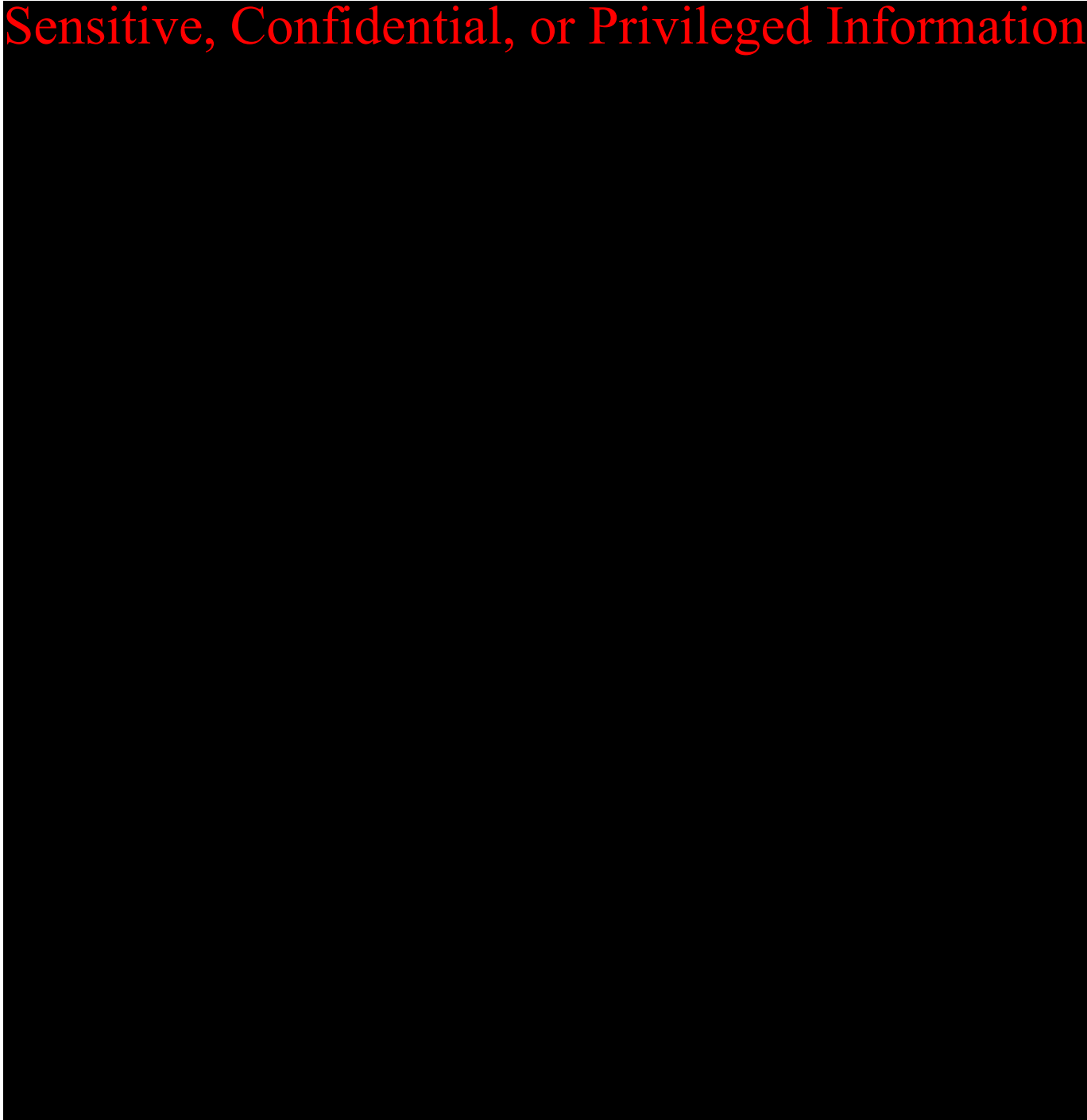
Figure 2-3: Mt. Simon Sandstone elevation map over the west-central portion of the Illinois Basin. Modified from FutureGen Alliance (2013).

Sensitive, Confidential, or Privileged Information
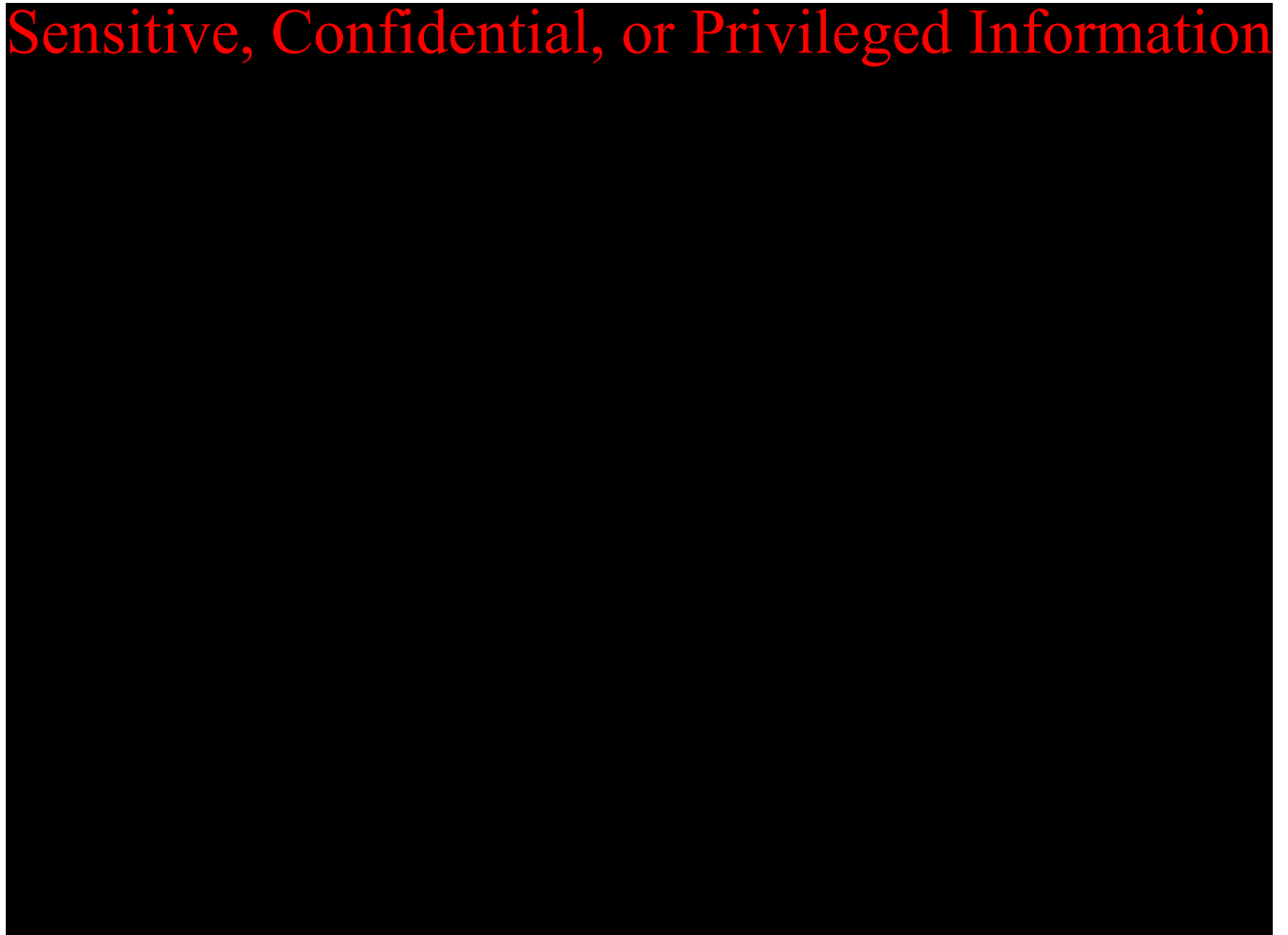
Figure 2-4: Mt. Simon Sandstone thickness map over the west-central portion of the Illinois Basin. Modified from FutureGen Alliance (2013).

Sensitive, Confidential, or Privileged Information

Sensitive, Confidential, or Privileged Information
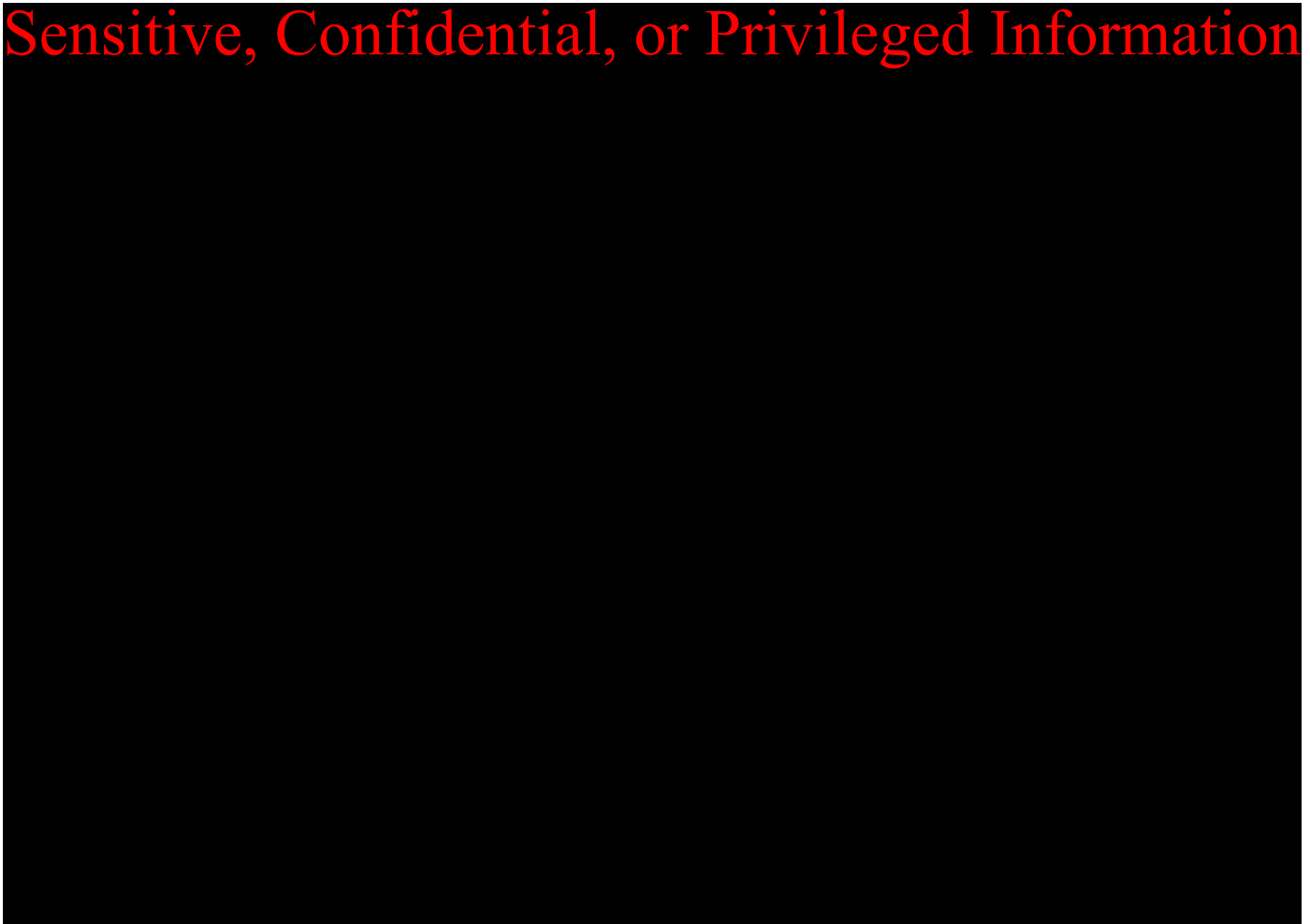
Figure 2-5: Eau Claire elevation map over the west-central portion of the Illinois Basin. Modified from FutureGen Alliance (2013).

Sensitive, Confidential, or Privileged Information
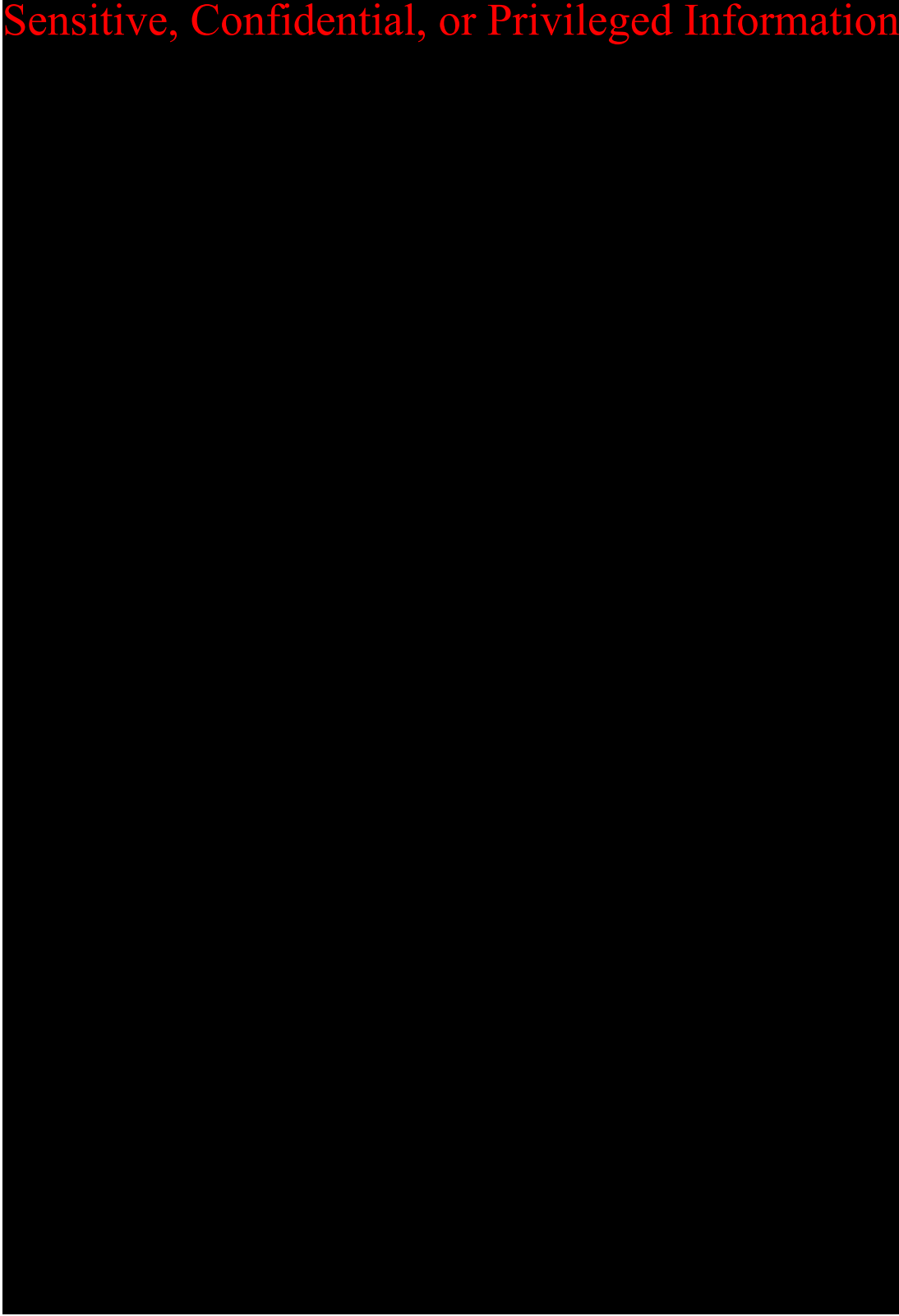
Figure 2-6: Eau Claire Eau Claire thickness map. Modified from Willman et al. (1975).

For the Marquis BioCarbon Project site, interpretations of the Mt. Simon's depositional setting were derived from work associated with the Illinois Basin Decatur Project site in Decatur, Illinois (Palkovic, 2015; Freiburg, 2020; Reesink, 2020), as well previous research on the UPH-3 well in Stephenson County, Illinois (Fischietto, 2009; Lovell, 2017). Previous research on these analog wells have detailed depositional environments, paleogeography, and Precambrian basement structure in the Illinois Basin. The proposed site location falls between these two data points (Figure 2-7), enabling on-site data to be correlated with regional interpretations.

Sensitive, Confidential, or Privileged Information
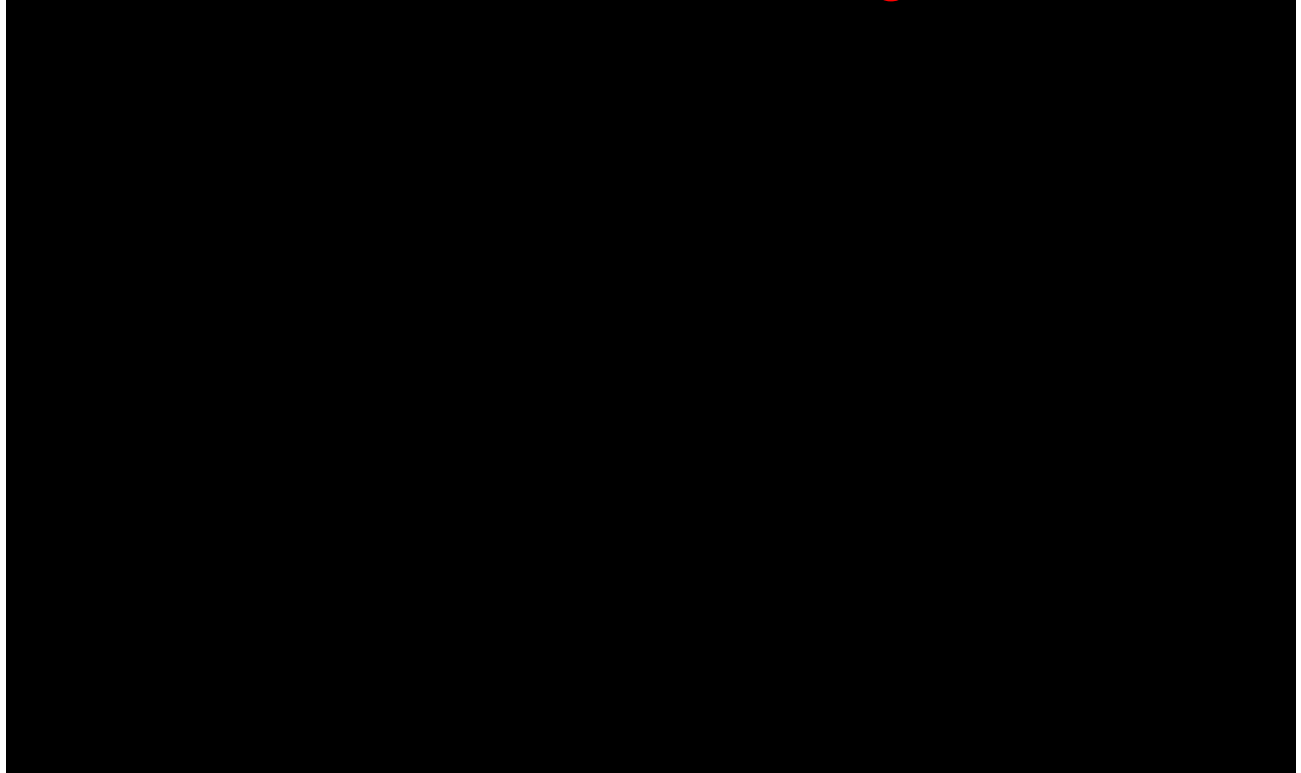
Figure 2-7: Map showing the analog well locations used in depositional environment interpretations to the north and south of the Marquis BioCarbon Project site.

Studying the composition of these core samples enabled an interpretation of lithofacies and depositional environments for the Mount Simon Sandstone in northern Illinois. During the Cambrian Period, a terrestrial fluvial environment of deposition transported sediments from topographically higher regions, such as mountains to the north (Wisconsin region), to a shallower region in Illinois. During transport, these sediments formed the Cambrian-aged depositional environments of the fluvial braid plains and eolian sand dunes (Figure 2-8).

Sensitive, Confidential, or Privileged Information
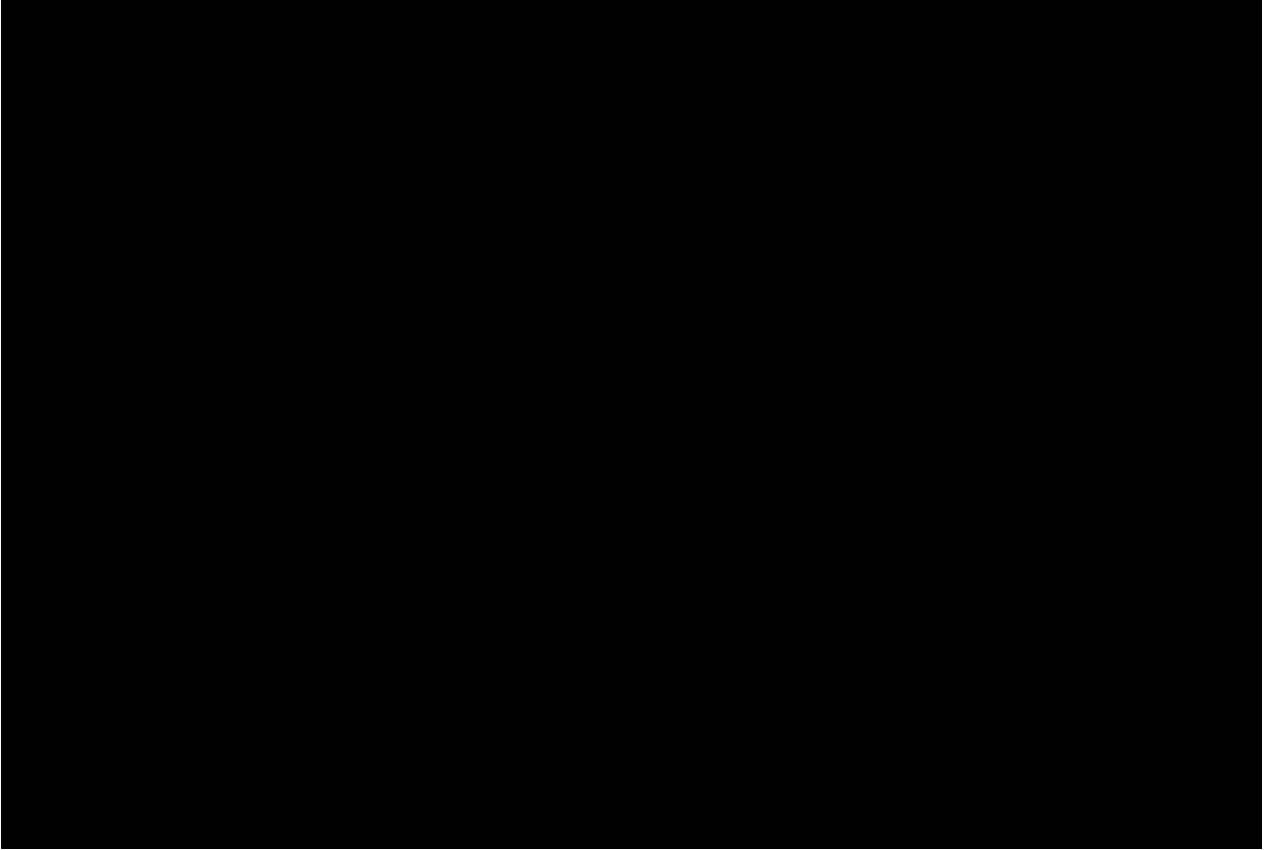
Figure 2-8: Regional depositional model for the Mt. Simon Sandstone. Broad fluvial braid systems feed into a shallow inland sea. Sediments on inactive braid plaids are reworked by eolian processes. Sediment source is primarily from the north. Modified from Fischietto (2009).

The Mt. Simon Sandstone can be divided into stratigraphic intervals associated with the timing and development of the basin that affects depositional settings. Core samples from the project site were integrated with regional studies, resulting in seven distinct depositional packages in the Mt. Simon (Figure 2-9). These environments include eolian sand dunes, fluvial braid plains, and braid deltas that transitioned into shallow marine depositional environments as sea level rose during deposition of the upper Mt. Simon and Eau Claire. Within the regional fluvial braid plain, there are playa (flat "ponding" areas) and eolian (dunal) sedimentary areas (Figure 2-10).

The Mt. Simon consists of sandstones that are generally clean, well-sorted, and porous. Variations in sediment grain size depend on how far sediments were transported from their source and whether they were reworked by wind (eolian sandstone), rivers and streams (fluvial systems), or water (shallow marine sandstones modified and sorted by wave action). At the Marquis BioCarbon Project site, the lower Mt. Simon consists of conglomerate and very coarse to fine-grained sandstone deposited by braided fluvial channels and eolian systems, as well as arkosic sandstones yielding high gamma ray values in Mt. Simon zones 5 and 6. In the Upper

Mt. Simon fluvial, tidal, and shallow marine depositional systems resulted in finer grained sandstone and increased clay content. During the deposition of the Eau Claire, shallow marine systems on the continental shelf deposited shales, siltstones, and fine to very-fine grained sandstones with dolomitic and arkosic compositions.
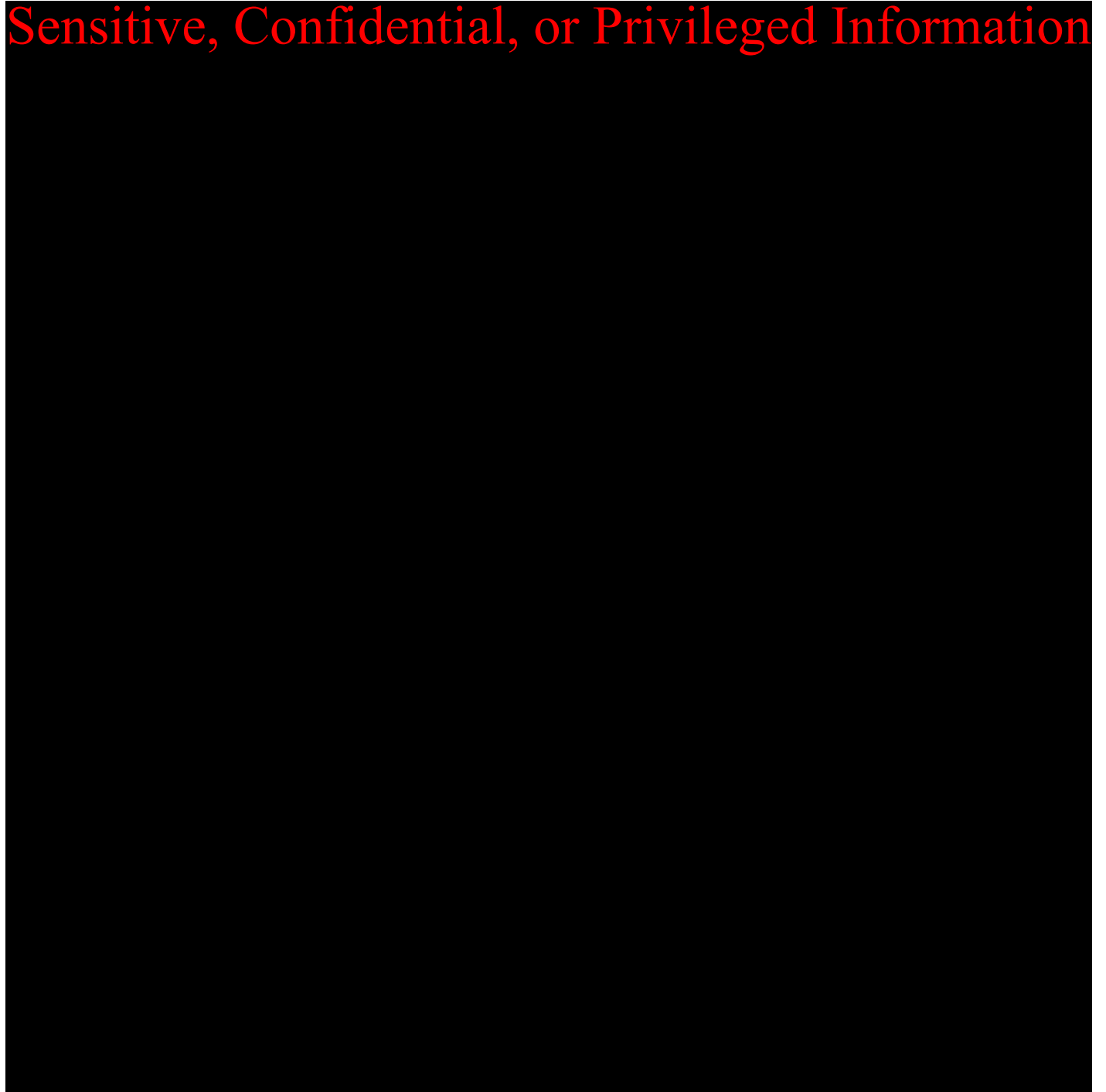
Figure 2-9: Interpreted Mt. Simon depositional environments and corresponding intraformational zones.

Sensitive, Confidential, or Privileged Information
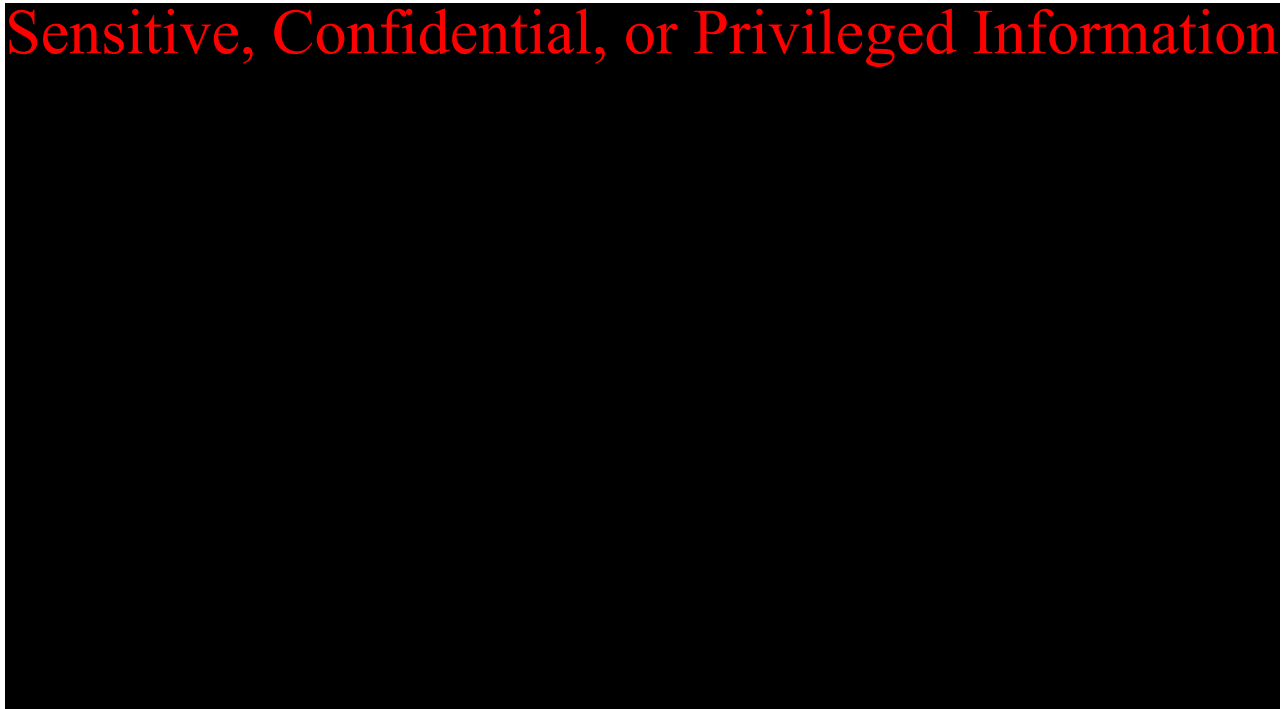
Figure 2-10: Example conceptual schematic drawing of the Mt. Simon Zone 5 representing the eolian depositional environment and interpreted orientations at the Marquis site (not to scale), as well as representative bedding features in whole core acquired from Mt. Simon Zone 5 (insert). Modified from Freiburg et al. (2020).

There are several geologic structures northeast of Putnam County (Figure 2-11). Within the Marquis BioCarbon Project AoR and Putnam County, these structures do not appear to have a significant impact on the confining zone and the target saline storage reservoir. The La Salle Anticlinorium is the dominant regional structure within the basin and has associated faults which cause varied relief of strata along its trend. This structure extends from La Salle County in north central Illinois to the southeast towards Lawrence County near Vincennes, Indiana. This feature is believed to be a drape fold or fault-propagation fold similar in structural style to monoclines that developed during the Laramide Orogeny in the western Unites States (Nelson, 1995). More than half of the La Salle Anticlinorium's uplift is believed to occur during Late Mississippian time, with the remaining uplift and nearby structural features occurring during the Pennsylvanian. There are small faults, anticlines, and domes near the La Salle Anticlinorium and along its trend. The Marquis BioCarbon Project site resides in an area fully removed from the anticline. Other structural features to the northeast of Putman County include the Ashton, Kankakee, and Wisconsin Arches, the Sandwich Fault Zone, and several minor synclines, anticlines, and domes (Golden StrataServices, 1984).
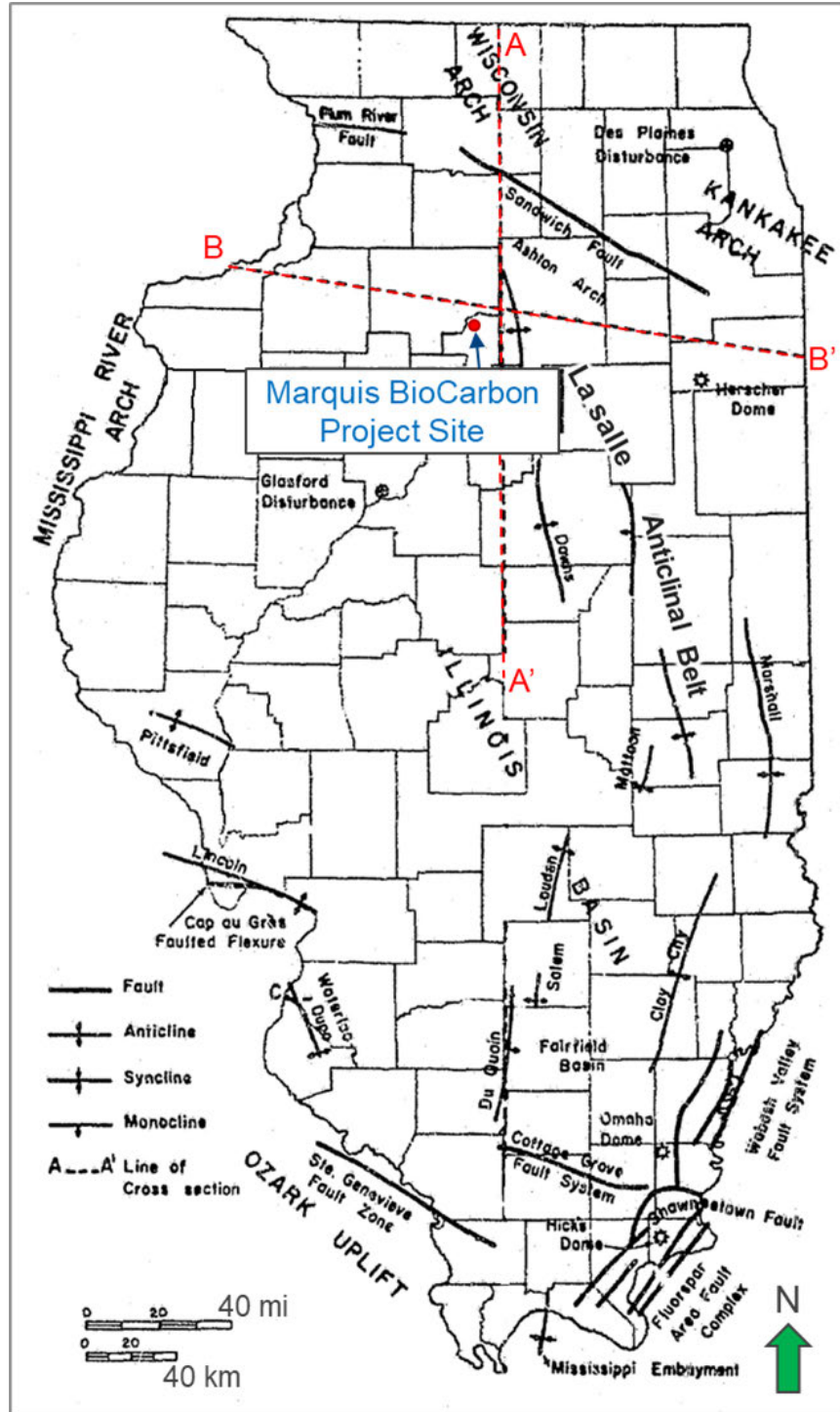
Figure 2-11: Principle geologic structures of Illinois. Modified from Willman et al. (1975) with N-S and E-W cross section marked in red. (See Figure 2-12 for cross sections)

Major geologic units and their stratigraphic relationships are depicted in regional cross sections shown in Figure 2-12. These two cross sections show the northward shallowing of Cambrian strata as well as the regional effect of the La Salle Anticline on the structural configuration of the
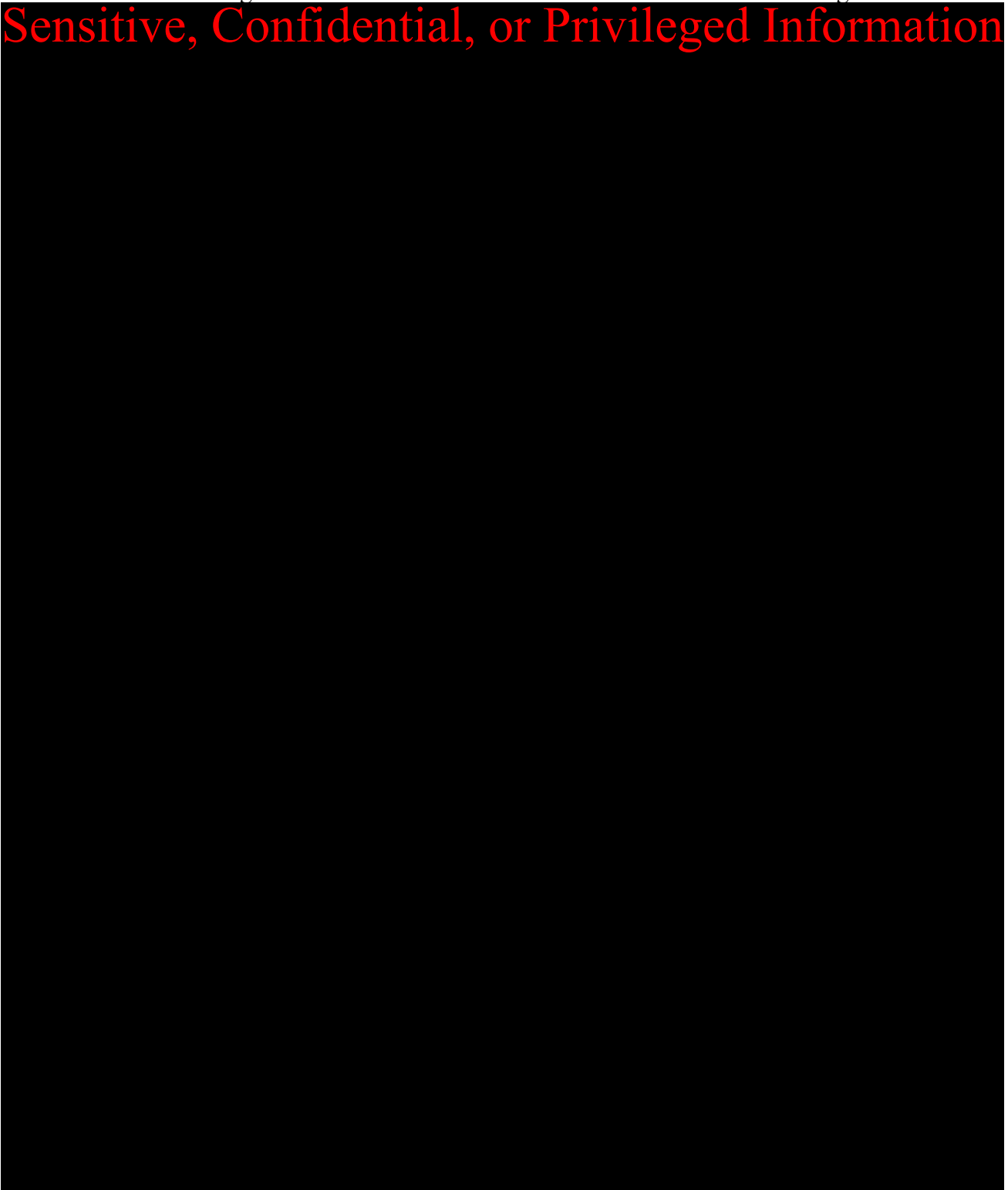
Figure 2-12: Geologic cross sections near Putnam County featuring the structural configuration of Cambrian strata that contains the target injection zone and caprock. The locations of these cross-section lines are shown in Figure 2-11. Modified from Willman et al. (1975).

2.1.3 Model Domain

A 49 mi^2 SEM centered on the Marquis BioCarbon Project site was used to assess potential CO_2 storage and estimate the extent of the CO_2 plume. To mitigate potential edge-effects in simulation, the 7-mi by 7-mi model grid was designed to encase the entirety of the plume and pressure front for the intended injection period. The grid size is set at 500 ft by 500 ft with an average of 10 ft layers in the injection zone and 12 ft layers in the confining unit. The model grid is centered around the MCI CCS 3 well, extending approximately 3.4 mi away from it in the X and Y directions. The proposed well location at the Marquis BioCarbon Project site is provided in Figure 2-13 and model domain information is summarized in Table 2-1.

Sensitive, Confidential, or Privileged Information
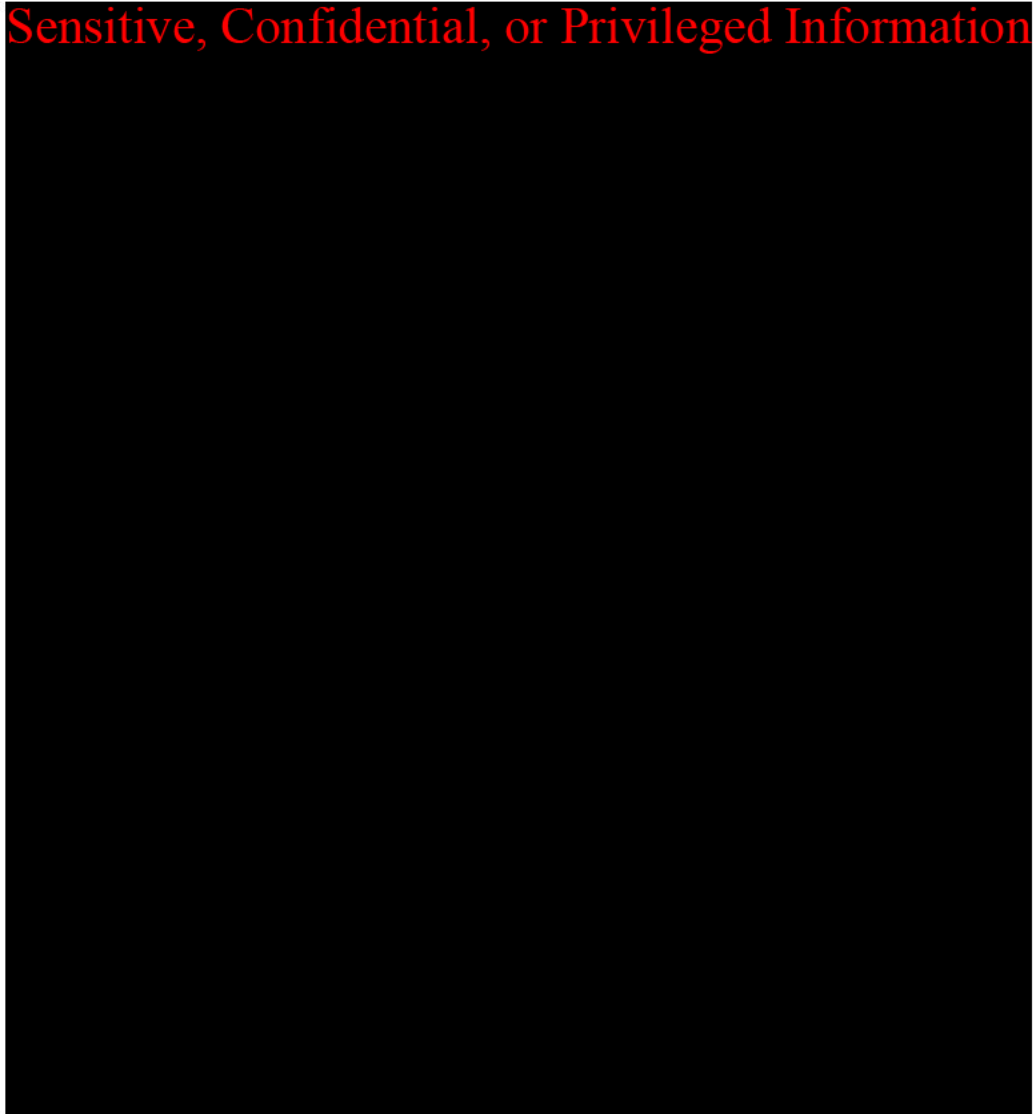
Figure 2-13: Static Earth Model 7-mile by 7-mile boundary centered around the MCI CCS 3 well.

Coordinate System	NAD 1983 BLM Zone 16N ft US		
Horizontal Datum	NAD83		
Coordinate System Units	Field = feet		
Zone	UTC -06:00 Central Time (US & Canada)		
FIPSZONE	1202		
Coordinate of X min	987293.52	Coordinate of Y min	14979542.23
Elevation of bottom of domain	-4473.32	Elevation of top of domain	-2117.49

Table 2-1: Model domain information.

The Mt. Simon sandstone is subdivided into seven internal zones based on observed responses seen in gamma ray and resistivity logs. These zones are numbered top down, as shown in Figure 2-14. While differently named, these zones are roughly equivalent to Mt. Simon subdivisions used in other studies and at other sites (Fischietto, 2009; FutureGen Alliance, 2013; Freiburg et al., 2014). Generalized reservoir quality of the zones indicates highest quality sands in the lower half of the formation, a middle section of lower-quality sands, and an upper section of higher quality, which is also a trend seen at the regional scale.

Sensitive, Confidential, or Privileged Information

Figure 2-14: Model Zones and corresponding gamma ray, resistivity, and porosity logs. Lower part of the Elmhurst and the entire Mt. Simon are considered reservoir, while the upper Elmhurst and Eau Claire shale act as the seal.

2.1.4   Porosity and Permeability

The geology of the injection interval was characterized based on depositional environments and subsequent controls on sand-quality distribution and implied flow geometries. Environments of deposition (EODs) were determined using paleogeographic information, results of well analyses of the Mt. Simon in analog studies (Fischietto, 2009; Freiburg et al., 2014), and rock observations in the whole core samples from the MCI MW 1 well.

EODs were defined on a zone-by-zone basis and incorporated into the model as objects representing channels and eolian sand deposits. These objects provided a way to constrain facies distribution throughout the model, where environmental controls on the deposition of clean sand and shale components could be represented. Facies used were defined with a clay fraction (vClay) log to separate the rock into three main types: clean sand, dirty sand, and shale. Each facies had a unique distribution of porosity values (Figure 2-15), which were utilized during the porosity property modeling process. Clean sand and dirty sand histograms had a distinctly different distribution in the Mt. Simon 2 and Mt. Simon 3 intervals, where normal distributions were centered around means which were shifted several porosity percentage points to the left (lower).

Figure 2-15: Histograms of porosity ranges by facies type showing correlative distributions for the clean sand, dirty sand, and shale facies. Distinctly different distributions for clean sand and dirty sand in Mt. Simons 2 and 3, where normal distribution means are lower.

The resulting porosity property (Figure 2-16a) was used as a direct input into the permeability property (Figure 2-16b), which was calculated in millidarcies (mD) using porosity-permeability transform functions derived from the nuclear magnetic resonance (NMR)-based permeability log. The NMR-based permeability values were cross-checked with core-measured permeability, and a strong correlation was shown (Figure 2-17). This provides confidence in the use of the NMR-based permeability log. The porosity-permeability function was applied based on flow-based facies, which were defined using a flow zone indicator (FZI) log.

The FZI data resulted in four additional "flow-based" facies types: high-flow sand, mid-flow sand, low-flow sand, and shale. Each lithofacies contained a component of each FZI and were subsequently divided into the corresponding amount of flow facies, which represented variabilities in pore-throat size and directly correlates to flow-potential. Two transforms were defined from this data: an upper transform for the high- and mid-flow sands, and a lower transform for the shale and low-flow sands (Figure 2-18). The final permeability property was cross-checked with well test results to ensure permeability height achieved in the model matched dynamic observations at the MCI MW 1 well.

Results of the property models reflect the degraded quality of the Mt. Simon 2 and Mt. Simon 3 relative to other zones. Conversely, the Mt. Simon 1, Mt. Simon 4, and Mt. Simon 5 were the highest quality zones. These relationships were considered when determining the well completions strategy, which is described in more detail in Section 2.2.

Sensitive, Confidential, or Privileged Information
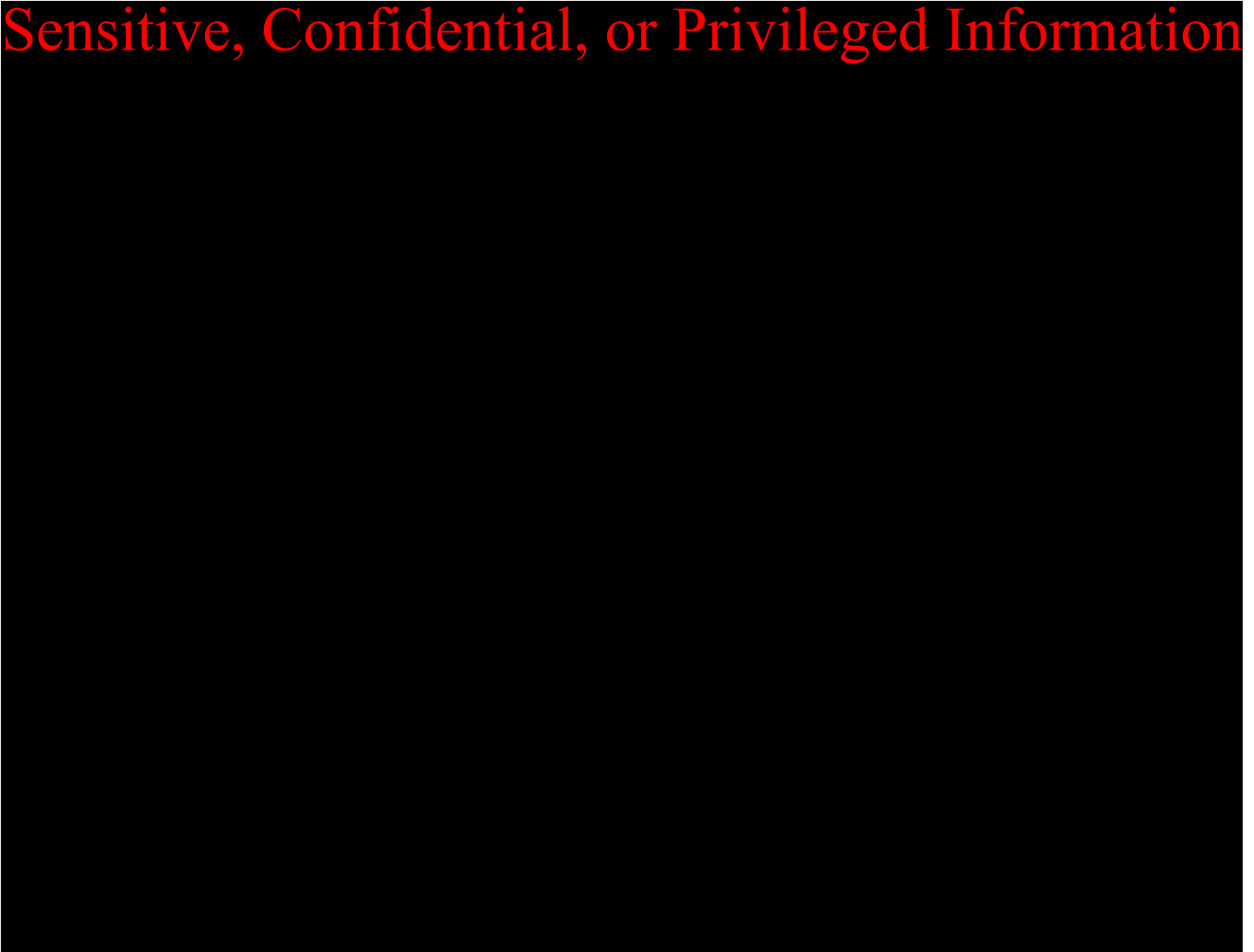
Figure 2-16: Final (a) porosity and (b) permeability properties showing the effect of depositional constraints on spatial property distribution within the 3D geocellular model.

Sensitive, Confidential, or Privileged Information
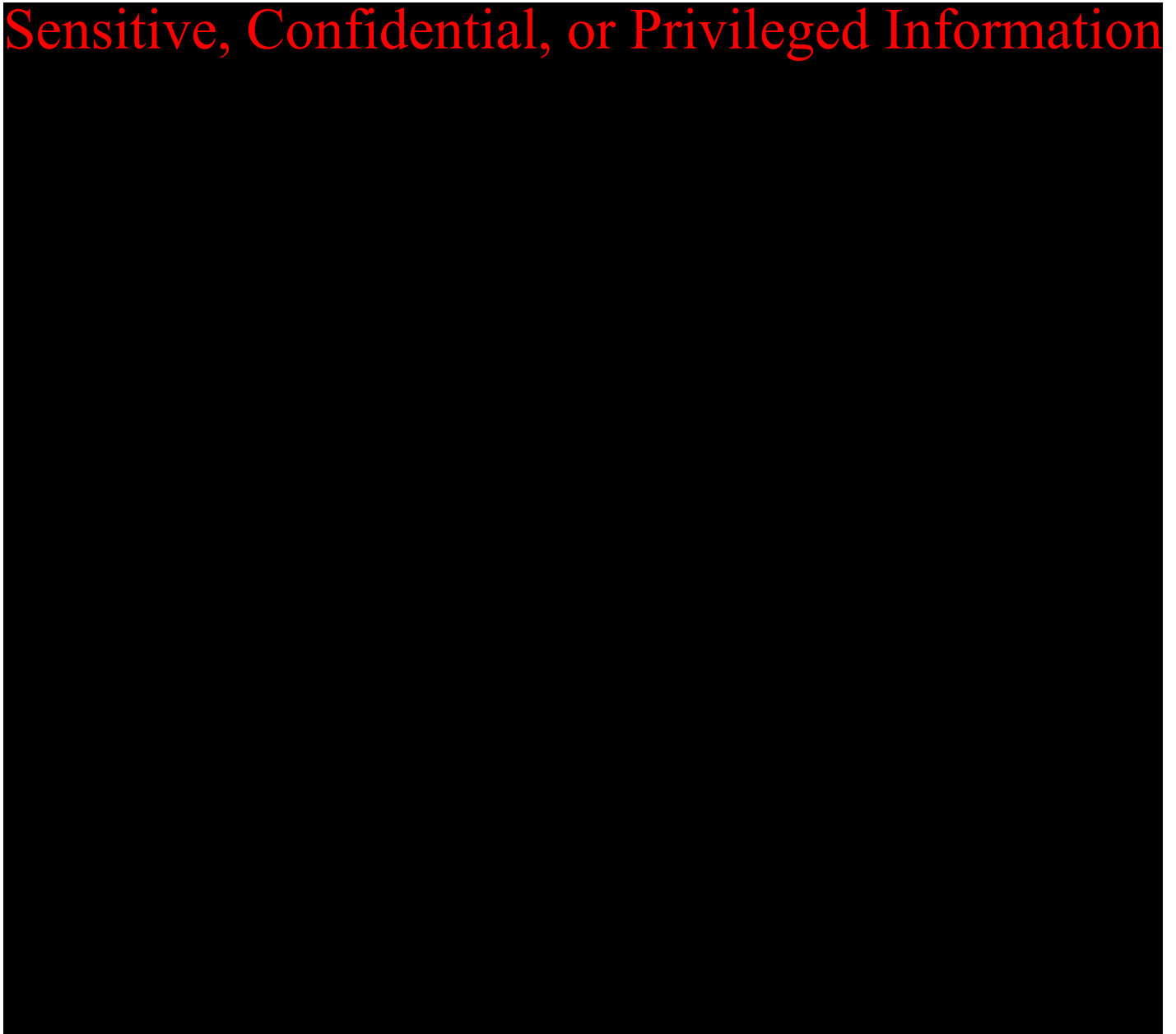
Figure 2-17: Logs at the MCI MW-1 well showing (left to right) gamma ray, stratigraphic zone, confining unit or injection interval, whole core, sidewall core, porosity, flow-based facies, and permeability. There is a match between the model (blocky colors) and the log (black line) for porosity and permeability, and core-measured permeability points plotted on the permeability track in magenta show strong correlation to NMR-based log values.

Sensitive, Confidential, or Privileged Information

Figure 2-18: Porosity-Permeability cross-plot colored by flow facies showing the utilization of two different transforms, applied by flow-based rock classifications.

2.1.5   Constitutive Relationships and Other Rock Properties

Relative permeability relationships served as the main constitutive relationships in the dynamic model. Relative permeability is an important input for describing dynamic behavior in reservoir simulators and it is a required property in the saturation equation describing multiphase flow in porous media. This flow property is represented as a saturation function and will significantly influence the simulated injection profiles. The curves incorporated in the model were from the CO_2-brine drainage relative permeability experiments performed by Core Laboratories on cores from the MCI MW 1 well. The steady-state method of measuring relative permeability was performed on three core samples taken at depths of 3,384.9, 3709.75, and 4,105 ft MD in the Mt. Simon Sandstone, producing three relative permeability drainage plots (Figure 2-19). Relative permeability versus saturation curves were assigned to facies in the dynamic model based on permeability and flow characteristics. Facies in the Mt. Simon Sandstone were categorized as "low-flow sand", "mid-flow sand" and "high-flow sand". The model assumed a compressibility of 1×10^{-6} 1/pound per square inch (psi), which is the average of the MCI MW 1 well pore volume compressibility log in the Mt. Simon. The log values were computed by Baker Hughes from geomechanics core tests and logs.

Sensitive, Confidential, or Privileged Information

Figure 2-19: Relative Permeability Curves imported into dynamic reservoir model. The plot on the left was assigned to high-flow sands, the plot in the middle was assigned to mid-flow sands and the plot on the right was assigned to low-flow sands.

2.1.6 Boundary Conditions

The model's lower boundary was the top of the Precambrian basement rock. While this surface is expected to have some topographical features, in general, it is assumed to dip to the southeast in the Putnam County area. The size of the static earth model was 7 mi × 7 mi. A single injection well was used at the center of the model so that the CO_2 plume and pressure buildup would be far from the computational model boundary (7 mi × 7 mi) and the model would be able to capture the multiphase flow phenomena. The model lateral boundary is assumed to be an infinite or open boundary reservoir. To model an open boundary reservoir, a volume modifier was used for the grids at the model boundary as recommended by CMG-GEM (CMG-GEM, 2016; Nghiem et al., 2009b).

2.1.7 Initial Conditions

Sensitive, Confidential, or Privileged Information

input in the simulator. Fluid density was calculated as a function of pressure, temperature, and salinity in the simulator.

Parameter	Value or Range	Units	Corresponding Elevation (ft MSL)	Data Source
Temperature	Sensitive, Confidential, or Privileged Information			Temperature Log
Pore pressure gradient				Drill Stem Testing
Fluid density				CMG Reservoir Simulator Calculation
Salinity				Drill Stem Testing

Table 2-2: Initial conditions.

2.1.8   Operational Information

Details on the injection operation are presented in Table 2-3.

	Operating Information	MCI CCS 3
Location (global coordinates)	X Y	41.27026520° -89.30939322°
Model coordinates (ft)	X Y	987293.52° 14979542.23°
Perforated interval (MSL)	Top Bottom	-3,226.14 ft -4,781.53 ft
	Wellbore diameter (in.)	9 5/8 inch
Planned injection period	Start End	01/01/2024 03/01/2029
	Injection duration	5 years
	Maximum injection rate	1.5 million tonnes (MT) /year

Table 2-3: Operating details.

2.1.9   Fracture Pressure and Fracture Gradient

Sensitive, Confidential, or Privileged Information

with literature and results from the hydraulic fracture tests performed in the FutureGen 2.0 site located in Morgan County, Illinois discussed in (Cornet, 2014).

Sensitive, Confidential, or Privileged Information

Injection Pressure Details	MCI MW 1
	Sensitive, Confidential, or Privileged Information
Fracture gradient	
Maximum injection pressure (90% of fracture pressure)	
Elevation corresponding to maximum injection pressure (MSL)	

Table 2-4: Injection pressure details.

2.2 Computational Modeling Results

2.2.1 Predictions of System Behavior

A 3D multi-phase flow simulator (CMG–GEM, 2021) was used to model CO_2 injection, determine the CO_2 plume position, and pressure front at the end of the injection period and during the post-injection period. The model includes target storage formations and confining zone formations. The geological model (SEM) that includes the permeability, porosity, and gridding of the model was imported from Petrel. The gas-water relative permeability relationship assigned to the model is described in Section 2.1.5.

Sensitive, Confidential, or Privileged Information
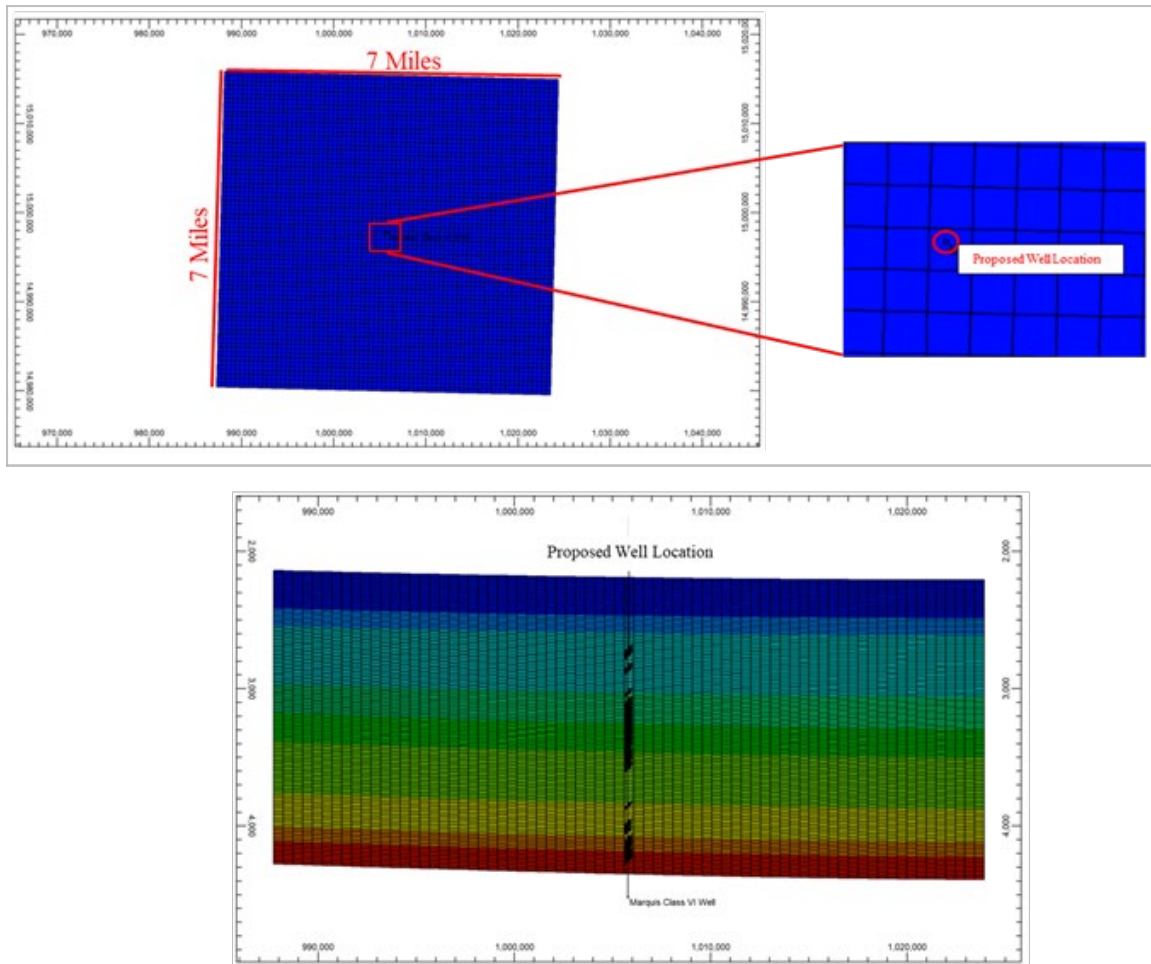
Figure 2-20: Map view of computational model with zoomed well grid (top) and cross section of the model (below).

The model demonstrates a 5-year injection period and 50-year post-injection period. The CO_2 injection rate was constrained to 1.5 MT/year.

CO_2 phase saturation is used as a defining parameter for the CO_2 plume extent. Figure 2-21 shows a side view of the CO_2 plume at the wellbore after 1, 3, and 5 years of injection. Figure 2-22 shows the same side view of the CO_2 plume at the wellbore at 3, 5, 10 and 50 years after the cessation of injection.

The CO_2 plume expands during the injection period and local permeability variations within the Mt. Simon Sandstone causes changes in the distribution of the CO_2 plume. At no time either during or after injection does the CO_2 migrate toward the top of the Mt. Simon.
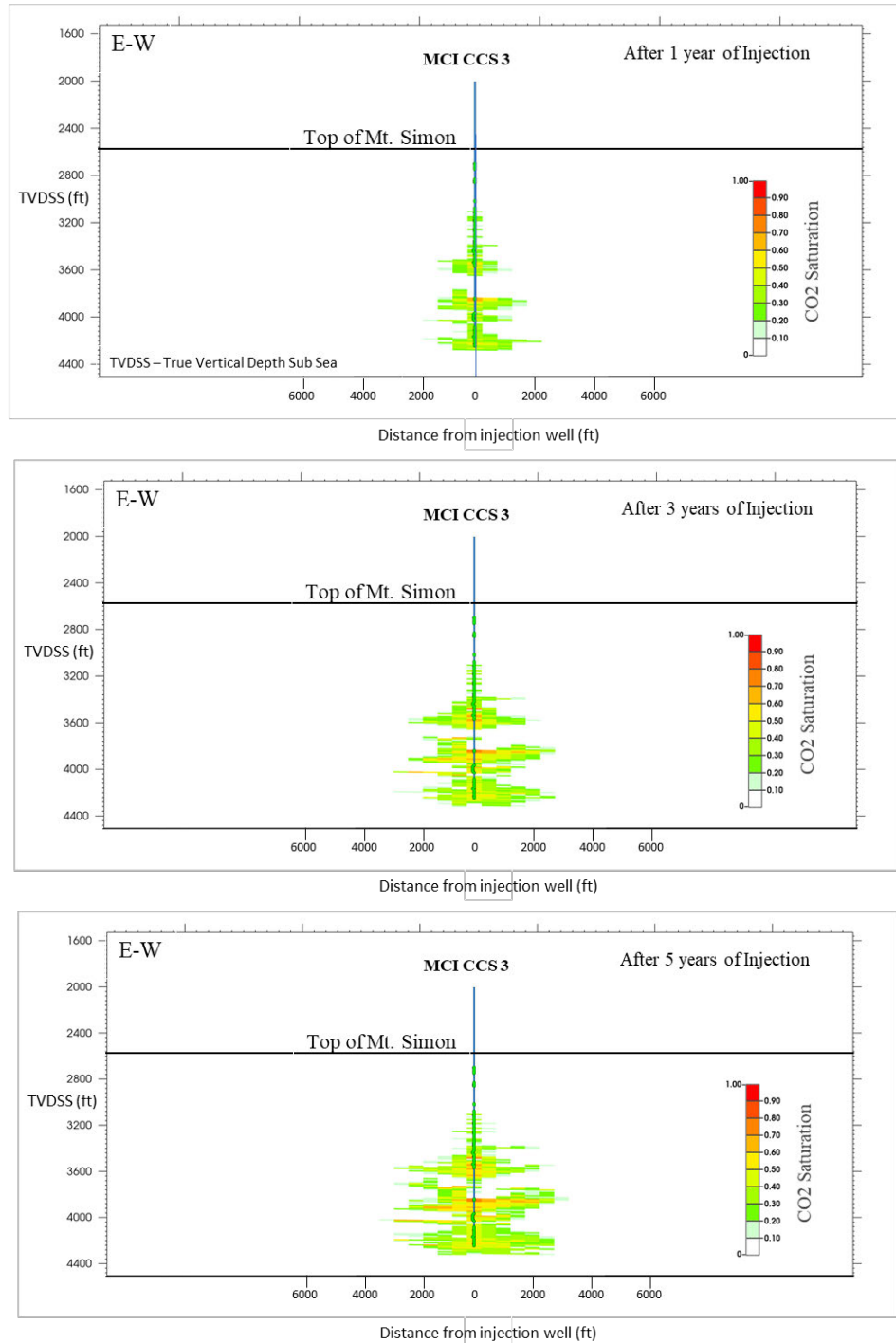
Figure 2-21: Development of CO_2 plume after 1 year (top), 3 years (middle), and 5 years (lower) of injection.
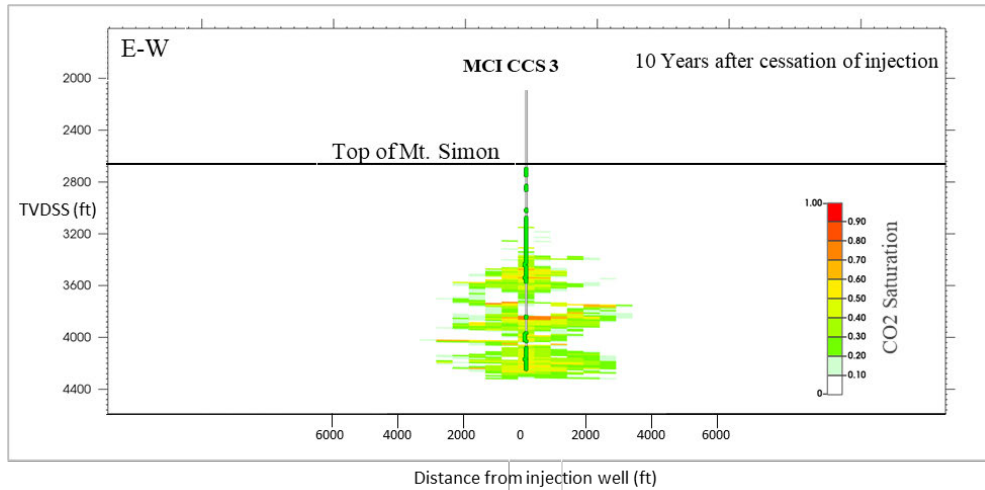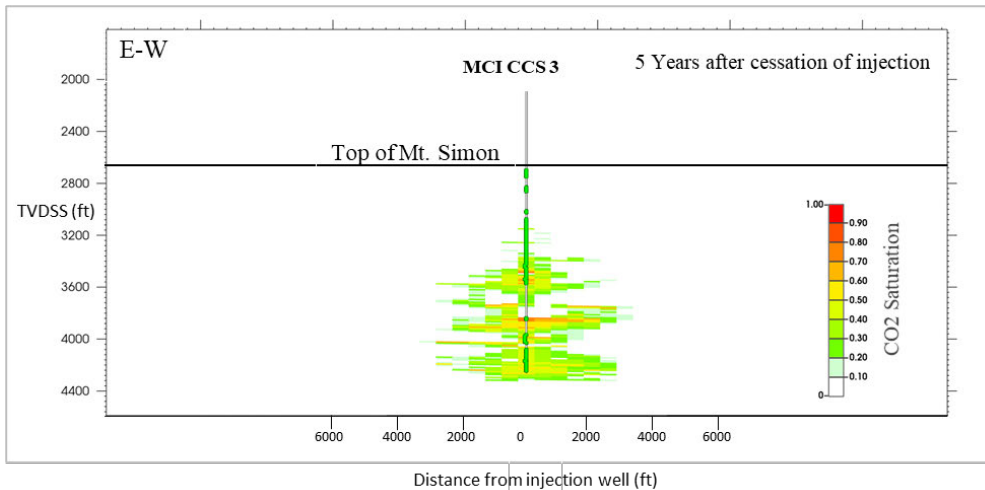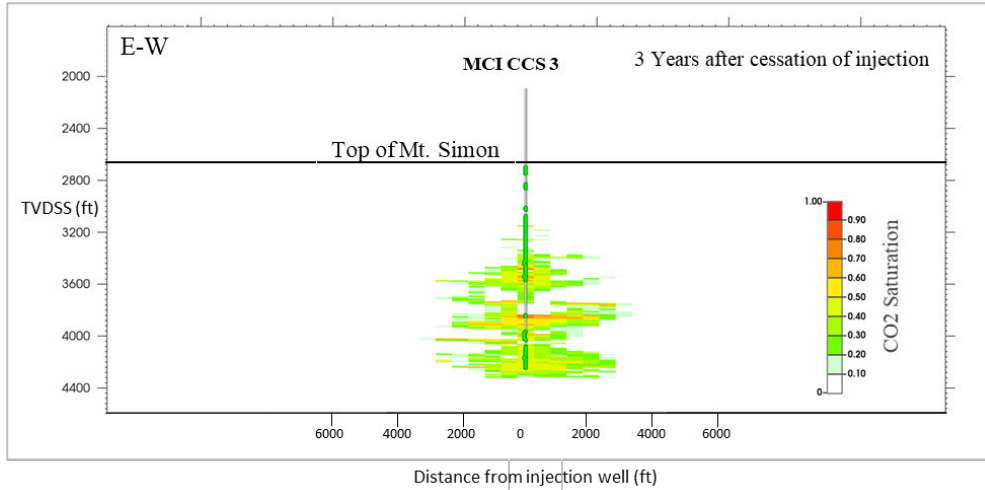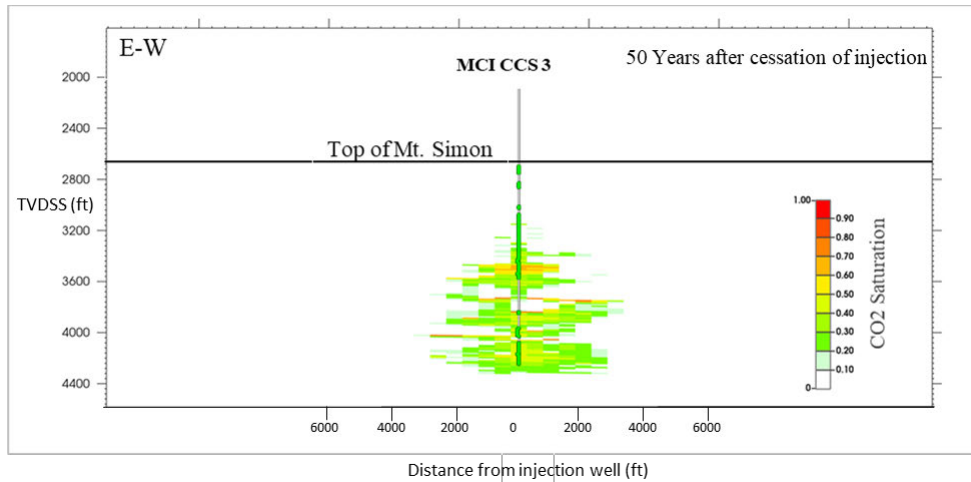
Figure 2-22: CO_2 plume 3, 5, 10 and 50 years after cessation of injection.

The CO_2 plume size after 5 years of injection for four different layers is shown in map view in Figure 2-23.

The AoR is determined by using the average plume sizes for all layers in the model at the end of the 5-year injection period which corresponds to layer 153. The CO_2 saturation in that layer at the end of injection period was selected to define AoR.

Figure 2-24 shows the development of the CO_2 plume size after 1, 3, and 5 years of injection for layer 153. Figure 2-25 shows the CO_2 plume size in the post injection time frame and clearly indicates stabilization of the plume after the cessation of injection.
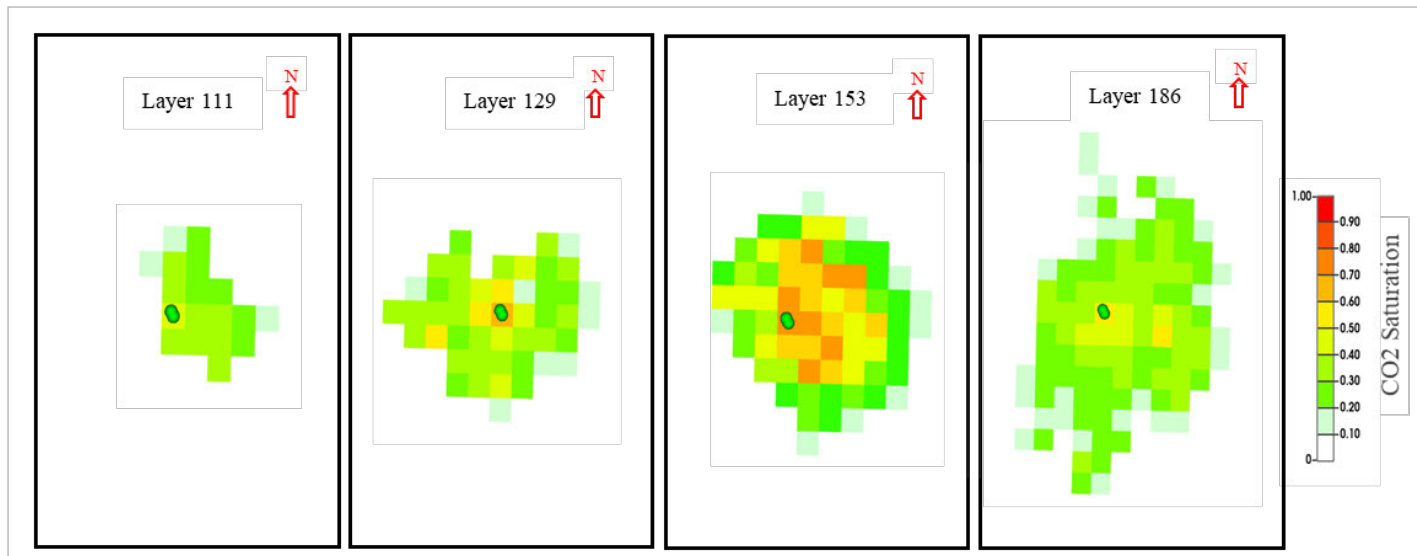
Figure 2-23: CO_2 plume after 5 years of injection in plan view for layers 111, 129, 153 and 186.
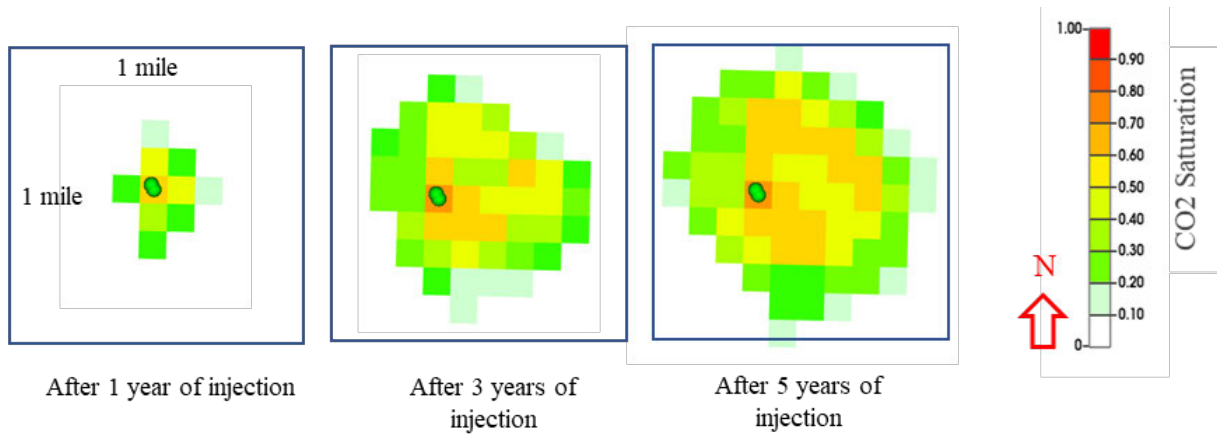
Figure 2-24: Development of CO_2 plume after 1 year, 3 years, and 5 years of injection at layer 153 representing the AoR.
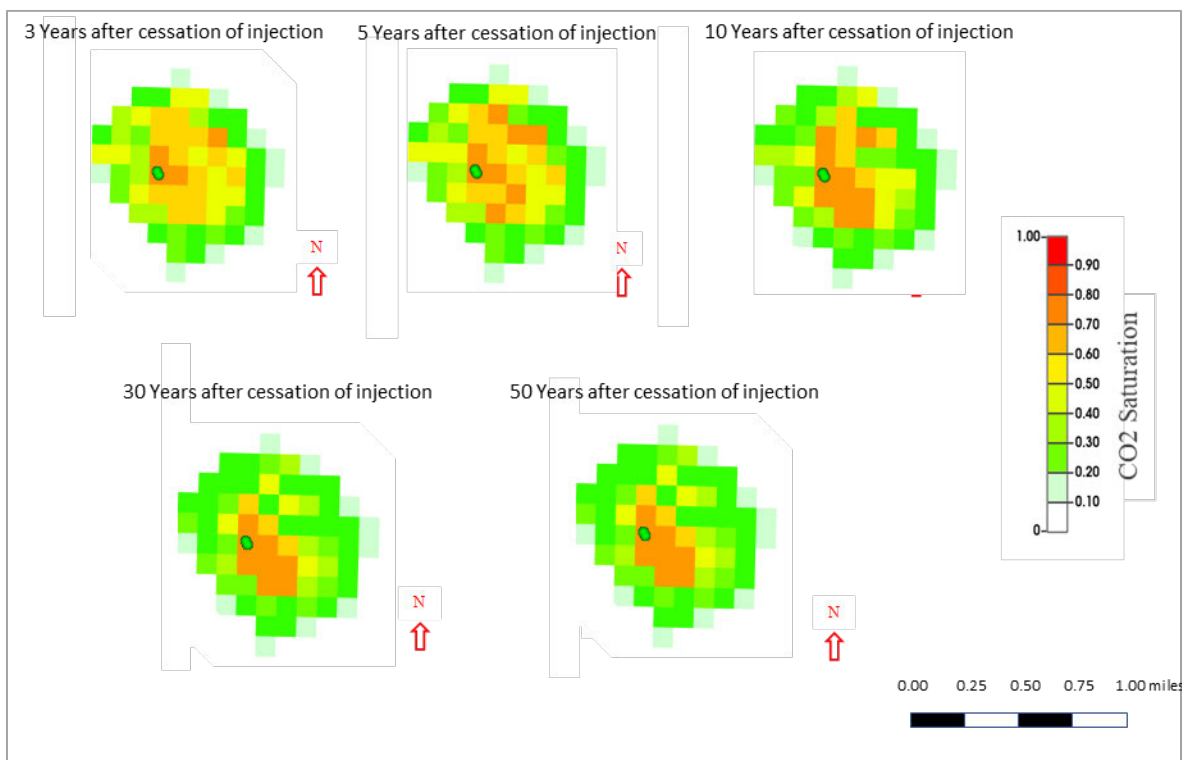
Figure 2-25: CO_2 plume mapping 3 year, 5 years, 10 years, 30 years, and 50 years after cessation of at layer 153 (representing the AoR).

Figure 2-26 shows the pressure build-up (increase from initial pressure) in the Mt. Simon formation after 1, 3, and 5 years of injection. A pressure cut-off of 150 psi was used in the plot to delineate pressure front expansion as a function of injection time as detailed in section 2.3.

Figure 2-27 shows the pressure time-series at the depth of the middle perforation. The pressure remains lower than the maximum injection pressure and declines rapidly after injection ceases.
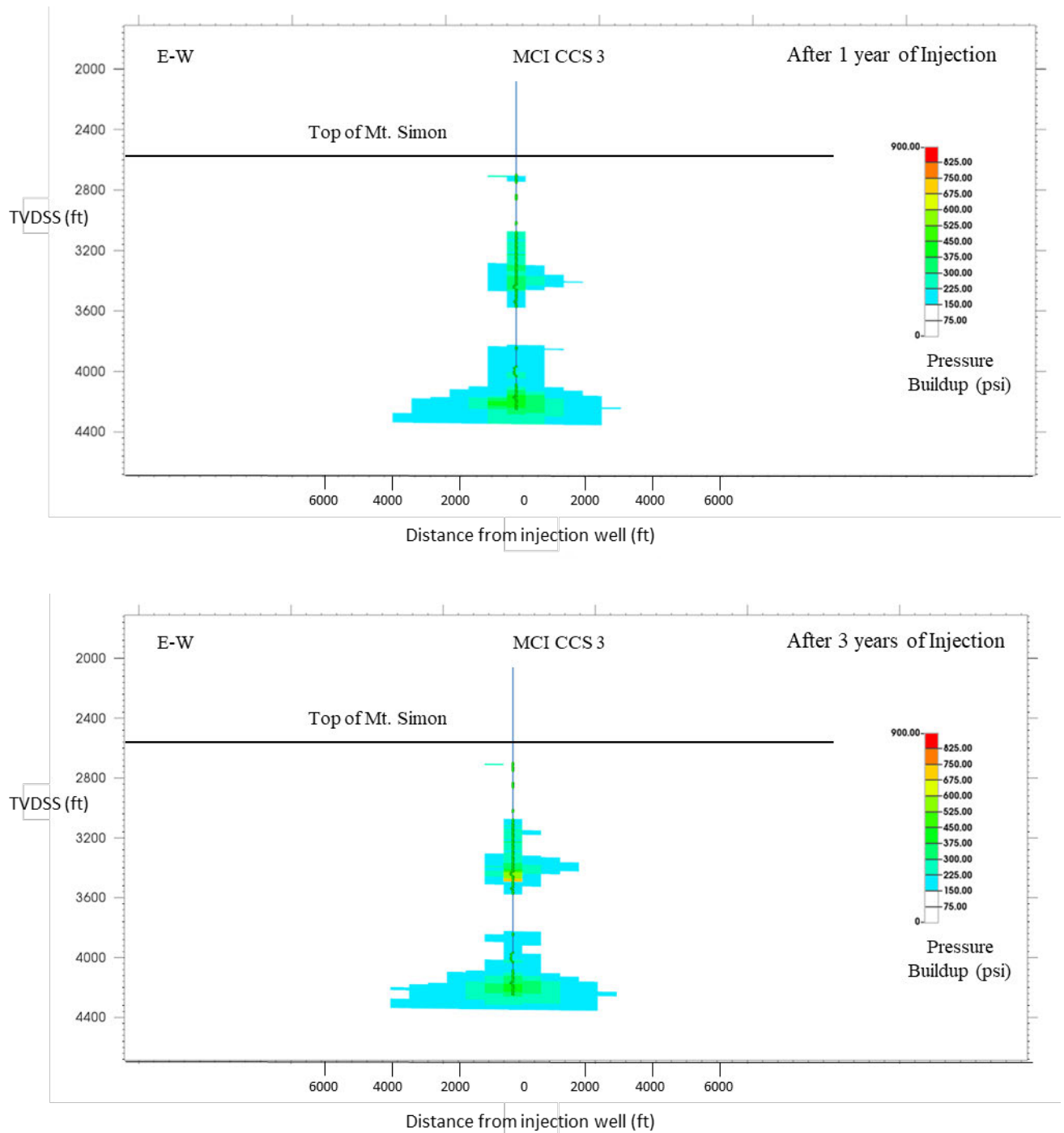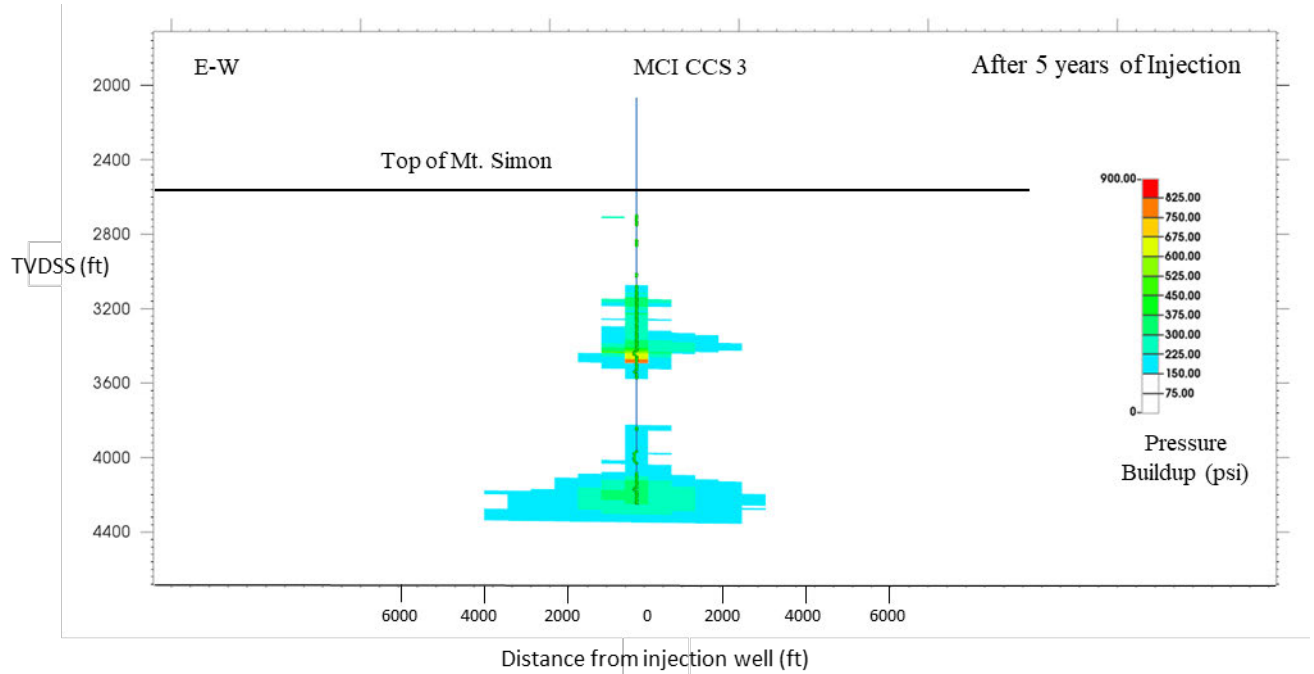
Figure 2-26: Pressure front after 1, 3 and 5 years of injection using 150 psi pressure cut-off.
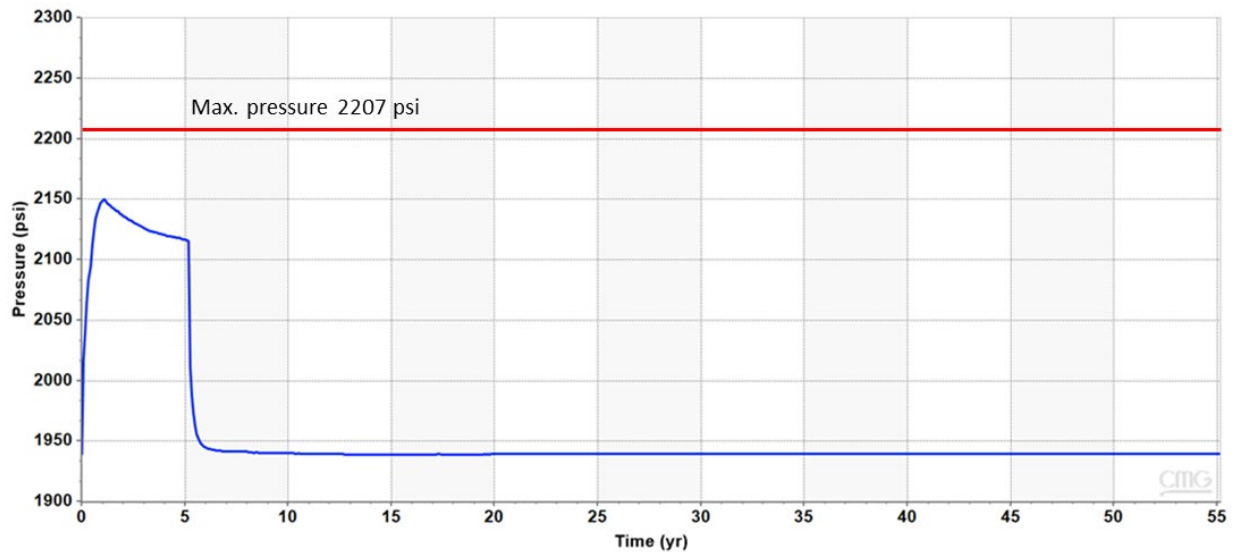
Figure 2-27: Pressure time-series data during injection and 50 years of post-injection period at depth of middle perforation (model layer 109, 3,898 TVDSS, ft.)

CO_2 saturation and pressure build-up were also modeled at the monitoring well location (MCI MW 2). The pressure at layer 153 (3,833 ft Subsea true vertical depth [TVDSS]) for the MCI CCS 3 and MCI MW 2 wells is plotted in Figure 2-27. As expected, the pressure build-up at the MCI MW 2 well is lower than the MCI CCS 3 well, and pressures quickly decline after injection stops.

Figure 2-29 shows the development of the CO_2 plume in layer 153 at the MCI CCS 3 and MCI MW 2 well. The CO_2 saturation immediately increases at the MCI CCS 3 well location compared to the MCI MW 2 well location.
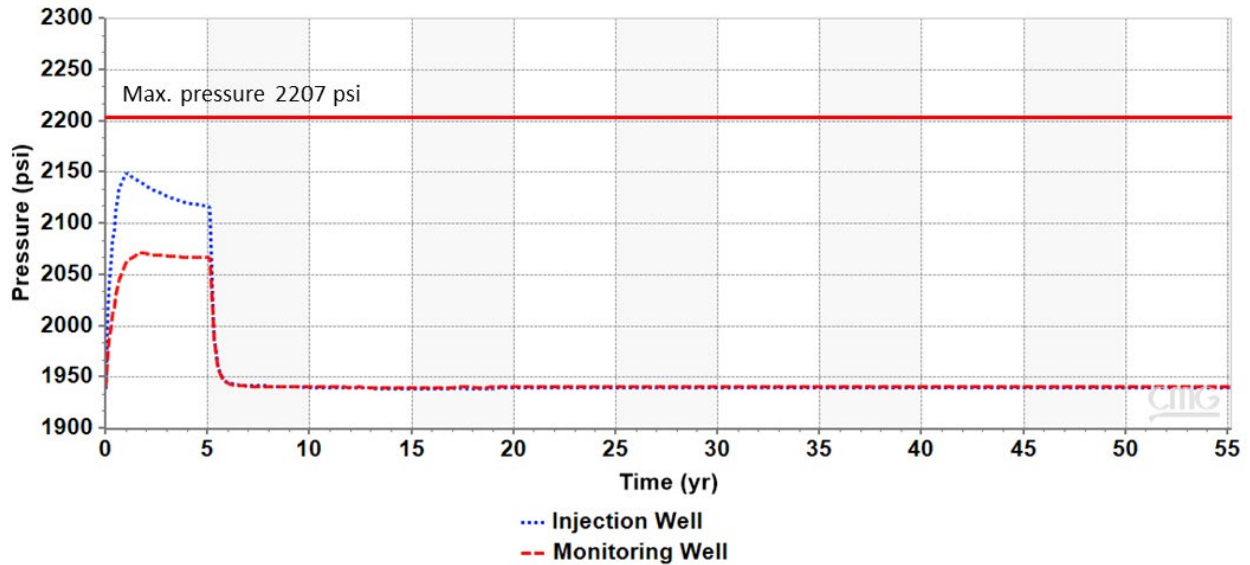
Figure 2-28: Pressure time-series data during injection and post injection period for monitoring (MCI MW 2) and injection well (MCI CCS 3) location at layer 153, 3,833 TVDSS, ft
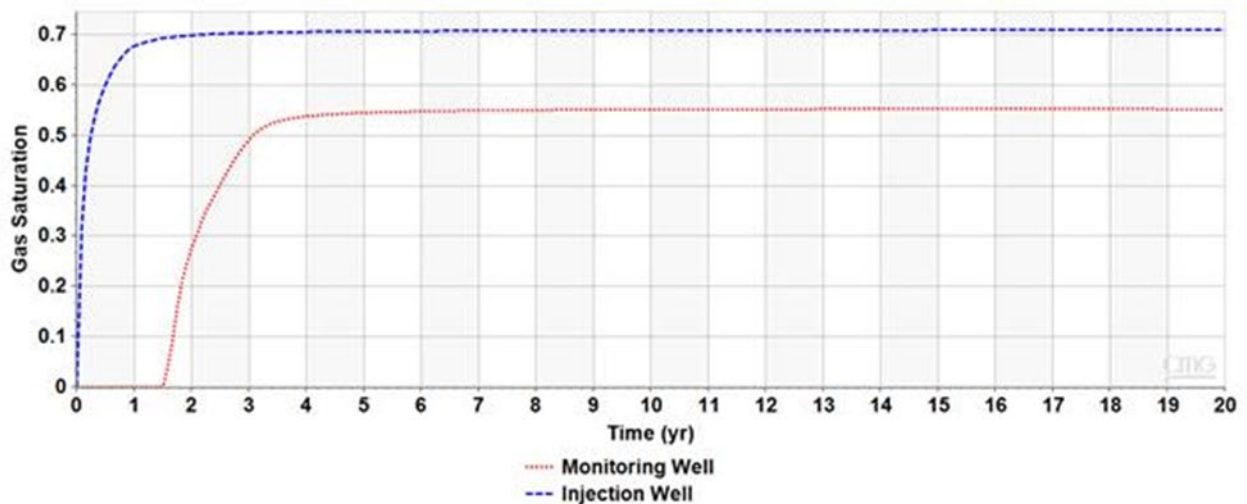
Figure 2-29: CO_2 saturation time-series data during injection and post injection period for monitoring (MCI MW 2) and injection (MCI CCS 3) well locations at layer 153 with MSL of 3,833 ft

2.2.2 Model Calibration and Validation

A robust earth model has been built and calibrated using data acquired in the MCI MW 1 well. Geological parameters (e.g., porosity, permeability), fluid flow data (e.g., relative permeability), and initial reservoir data (e.g., temperature, initial pressure gradient, fracture pressure gradient) used to build the computational model, were derived from data collected from the well. A wide variety of data was acquired from logs, core tests and other field measurements such as minifracs and drill stem tests (DSTs). The data acquired greatly enhances the geologic knowledge of the area confirming the characteristics of the site as a viable storage site.

Planned wellbore parameters such as tubing size and tubing temperature profile were also incorporated in the model for additional accuracy. Once the injection phase of the project begins, the monitoring data such as pressure and injected rates will be used to calibrate, and history match the model as the project proceeds. Moreover, as described in section 2.4 (below), the AoR will be assessed during the lifetime of the project.

Subsurface uncertainty is also addressed through the creation and simulation of alternative geological scenarios. Sensitivity runs were performed for different porosity and permeability relationships as shown in Figure 2-30. All model parameters were the same as the base case apart from the porosity and permeability.

Figure 2-30: Porosity and permeability relationships for high side case (orange line) and low side case (blue line) showing an inverse relationship between the two scenarios. The numbers on the orange are permeability values, number on the blue line are porosity values.

The plume side views for the base, high side and low side cases after 3 years of injection are compared in Figure 2-31. The low side case scenario results in a larger overall plume diameter compared to the other two cases. Figure 2-32 shows the CO_2 plume in map view at layer 153, at the end of injection period and 5 and 10 years after the injection stops for the base case scenario. Results of the sensitivity analysis (high side case and low side case) shown in Figure 2-33 for CO_2 plume at layer 153 show that the AoR is smaller compared to base case scenario at the end of injection and post injection. It is also shown in Figure 2-33 that the plume size in the high and low side scenarios remains unchanged after 1 year post injection.
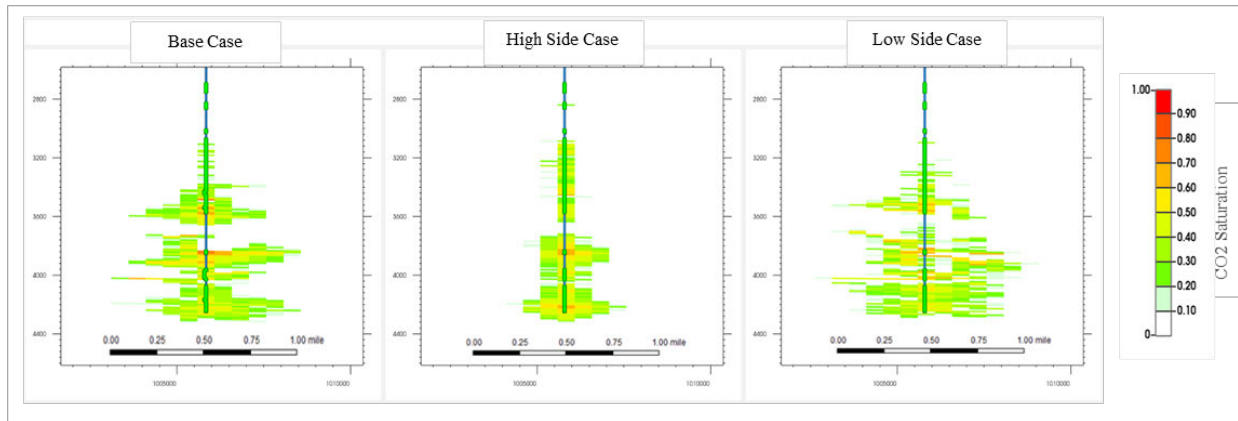
Figure 2-31: CO_2 plume at wellbore cross section after 3 years of injection. The left plume diagram represents the base case, middle represents the high side case, and the right plume diagram represents the low side case.
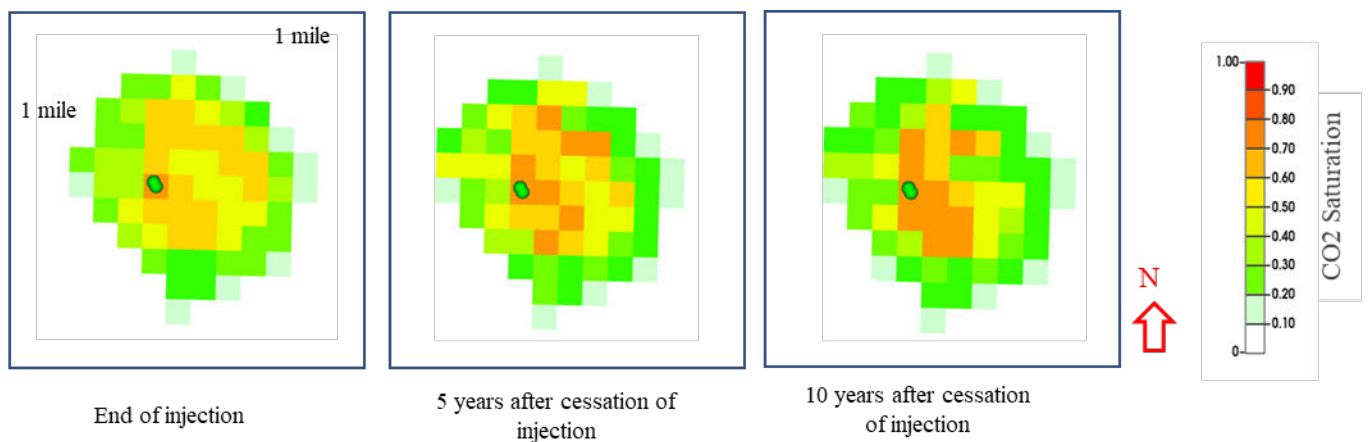
Figure 2-32: CO_2 plume at layer 153 (used to delineate AoR) for the base case at the end of injection, 5 years after injection stopped, and 10 years after injection stopped.
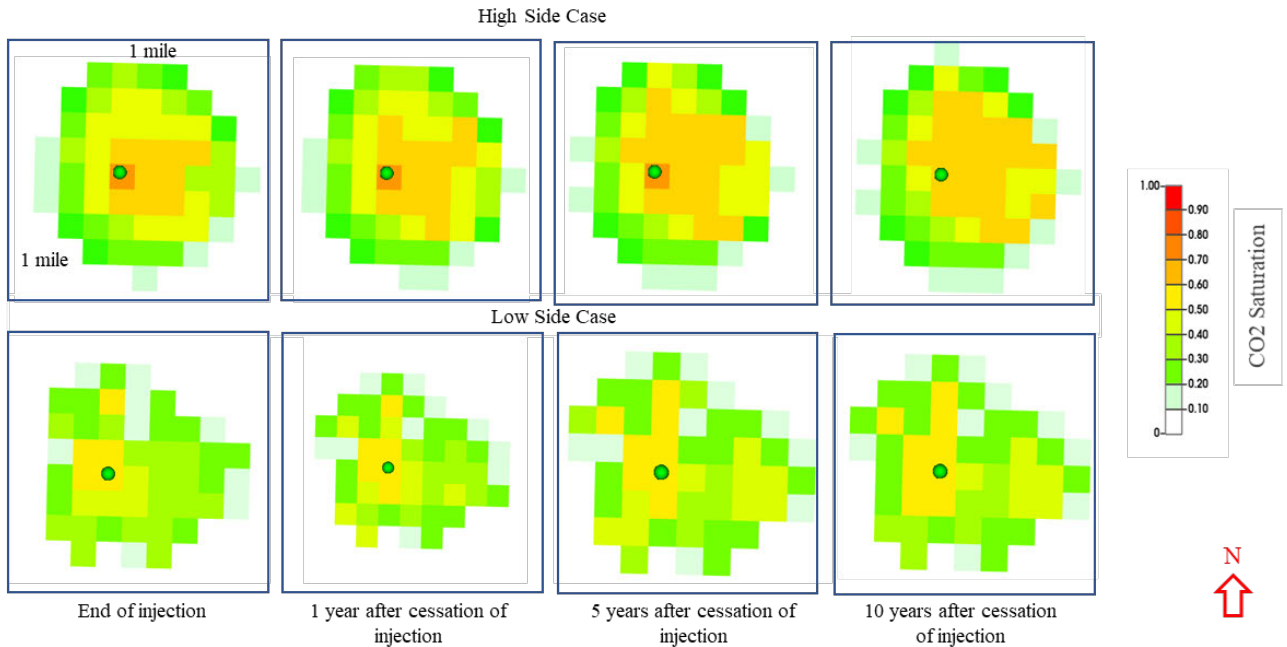
Figure 2-33: CO$_2$ plume at layer 153 (used to delineate AoR) at the end of injection and after, 1, 5 and 10 years after cessation of injection for the high side case (top row) and low side case (bottom row).

2.3 AoR Delineation

2.3.1   Critical Pressure Calculations

The critical pressure corresponds to the pressure needed to move fluids from the storage formation into a USDW through a hypothetical open conduit such as an uncemented well. Different methods can be used to calculate the required pressure to move fluid from the reservoir into a USDW. A simple hydrostatic head calculation (density of injection zone brine × depth distance between lowest USDW and top of injection zone × gravity constant) was used to

Input Data (Available)		
Attribute	Zone	Value
Depth	Deepest known USDW (Gunter)	Sensitive, Confidential, or Privileged Info
	Top of the first injection zone (Mt. Simon Sandstone)	
Pore pressure gradient (to estimate pressure)	All zones	
Input Data (Calculated)		
Attribute	Zone	
Pressure	USDW	
	Topmost injection zone (Mt. Simon Sandstone)	

Table 2-5: Input data used for critical pressure calculation.

2.3.2   AoR Delineation

For the purposes of AoR determination, the extent of the CO_2 plume has been assessed at each vertical layer of the storage reservoir in the computational model. As discussed above, the plume size at layer 153 represents the average plume size of all the layers during injection and post-injection. The AoR is established by expanding the plume by 0.25 mi in all directions. Figure 2-34 shows the CO_2 plume extent and AoR delineation predicted by the computational modeling during the project lifetime.

2.4 Corrective Action

2.4.1   Tabulation of Wells within the AoR

Wells within the AoR were identified using well databases held by the ISGS. Available well information indicates that wells inside the AoR are all shallow groundwater wells less than 220 ft MD. A total of seven water wells are present within the AoR. Table 2-6 details these wells and includes the locations, dates drilled, total depths and aquifer depths, and compositions of the

API Number	Latitude	Longitude	Date Drilled	Total Depth (ft)	Total Depth Lithology	Bedrock top depth (ft)	Aquifer Top Depth (ft)	Aquifer Bottom Depth (ft)	Aquifer Description	Static Water Level (ft)

Sensitive, Confidential, or Privileged Information

Lithology Key: SH = shale, CL = clay, S = sand, SG = sand & gravel.

Table 2-6: Tabulation of wells within the AoR

Sensitive, Confidential, or Privileged Information
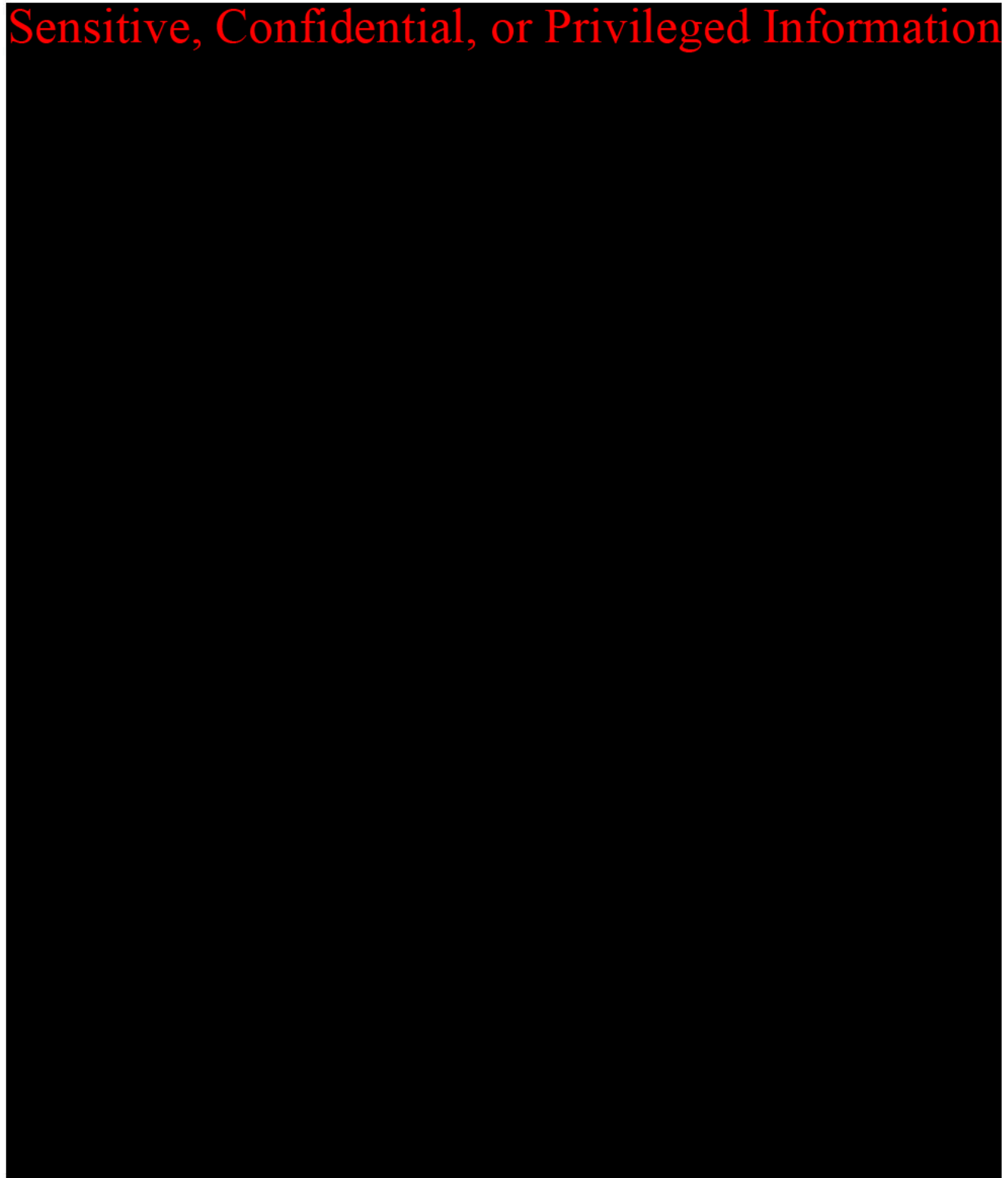
Figure 2-34: Map showing the modeled CO_2 plume footprint, AoR, and existing and proposed project wells within the AoR. Well data is summarized in 2-6.

2.4.2   Wells Penetrating the Confining Zone

Sensitive, Confidential, or Privileged Information

2.4.3   Plan for Site Access

Sensitive, Confidential, or Privileged Information

2.4.4   Corrective Action Schedule

It is not expected that any of the groundwater wells in the AoR will require corrective action. No corrective action schedule has been developed due to the absence of wells penetrating the confining zone within the AoR. The AoR will be re-evaluated every five years during the injection and post-injection phases unless an event occurs that triggers an AoR re-evaluation sooner. If the results of testing and monitoring and/or AoR re-evaluation throughout the project lifecycle indicate potential interference with any wells penetrating the confining zone, an amended corrective action plan will be implemented and submitted to the EPA (40 CFR 146.84 (e)(4)).

2.5 Re-evaluation Schedule and Criteria

2.5.1   AoR Re-evaluation Cycle

Marquis BioCarbon Project will re-evaluate the above described AoR every five years during the injection and post-injection phases pursuant to 146.84 (e).

The workflow (procedures) for incorporating the new data into the models as the project progresses is detailed in Figure 2-35.
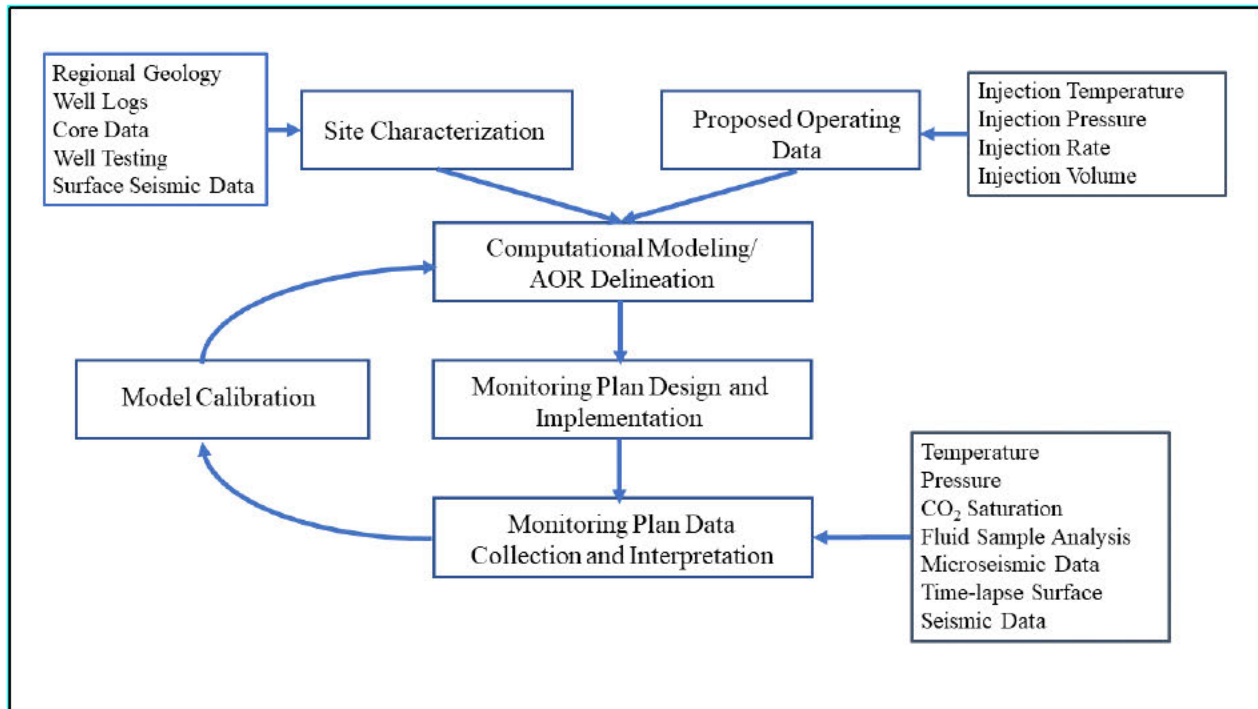
Figure 2-35: Workflow used to update the SEM and computational modeling.

With new data, model refinement is anticipated. The comparison of the original modeling with the updated modeling can take the form of several key evaluation metrics. This includes a comparison of:

- Changes to the static CO_2 resource estimate

- Differences in CO_2 plume geometry and volume

- Changes in pressure response

Any updates to the AOR will include an assessment of any additional wells that might be in the re-evaluated AoR that may need corrective action as well as an amended AoR and corrective action plan (40 CFR 146.84 (e)).

Once the injection phase of the project commences, both operational and verification monitoring data will be used to calibrate and update the computational model. Figure 2-35 illustrates the workflow and data inputs used to inform and calibrate the computational modeling. Operational monitoring data will be recorded on a continuous basis through the injection phase of the project. Pressure sensors located in the Mt. Simon Sandstone in the MCI MW 2 well will be retrieved on a quarterly basis for data download. In addition, pulsed neutron logs will be acquired in the MCI MW 2 well on a yearly basis to monitor CO_2 saturations along the well bores. The pressure and CO_2 saturation data from the MCI MW 2 well will be particularly useful in calibrating the computational model, as it will provide data on how the pressure plume is propagating through the Mt. Simon Sandstone away from the injection well. Computational model updates are also

expected to occur when the time-lapse surface seismic data are acquired on a four-year schedule. For more details on the Testing and Monitoring Plan and schedule refer to Permit Section 7.

The computational modeling will be updated with the downhole pressure and operational monitoring data on a quarterly basis for the first year of injection. If the system stabilizes, model updates will be scaled back to semi-annual updates to coincide with EPA reporting requirements (40 CFR 146.01). Any significant divergence of the monitoring data from the model predictions will be identified during the regular model updates and investigated. Model calibration with early monitoring data is expected to improve model predictions over the course of injection. It should be noted that model history-matching and calibration are not expected to trigger AoR reevaluations on a regular basis.

2.5.2   Triggers for AoR Reevaluations Prior to the Next Scheduled Reevaluation

The AoR will be updated on a 5-year schedule. However, Marquis Carbon Injection LLC will discuss any events that could impact the AoR with the UIC Director to determine if an AoR re-evaluation is required. If an unscheduled re-evaluation is triggered, Marquis Carbon Injection LLC will perform the steps described at the beginning of this section of this Plan. A report will be submitted to the UIC Director within 90 days of the AoR re-evaluation.
Monitoring and operational conditions that may warrant a re-evaluation of the AoR include (EPA, 2013):

- Changes in site operations that might alter the model predictions or the AoR delineation

- Site characterization data that may significantly change the computational model predictions and delineated AoR

- Monitoring results that indicate that the areal extent of the CO_2 plume or pressure front differ significantly from the model predictions

- Monitoring results indicate that the CO_2 has migrated beyond the confining zone

Table 2-7 details the operational changes and site characterization data that may warrant a reevaluation of the AoR. Table 2-8 specifies the observed changes and monitoring technologies that may trigger a re-evaluation of the AoR. Refer to the Testing and Monitoring Plan for more details on the proposed monitoring technologies for the project (Permit Section 7).

Area of Change	Variable
Operational Changes	• Increase in number of Class VI injection wells injecting in the Mt. Simon Sandstone in the immediate project area • Increase in CO_2 injection rates or volumes • Injection pressures more than the maximum allowable injection pressure for the project
Site Characterization Data	• Identification of a potential conduit for CO_2 or brine migration through the confining zone • Further characterization of storage formation heterogeneity that significantly effects CO_2 and pressure plume development

Table 2-7: Changes in operations and site characterization that may trigger AoR re-evaluation.

Observed Change	Monitoring Technology
Significantly larger pressure increases in the Mt. Simon Sandstone in the monitor well than were predicted by the model	Pressure sensors
Early breakthrough of CO_2 at the monitor well	Fluid sampling Pulsed neutron logging
CO_2 plume expands much faster than predicted by model	Time-lapse surface seismic data
Sustained pressure increases observed in above confining zone (ACZ) monitoring intervals	Pressure sensors
Geochemical changes in the ACZ monitoring intervals indicate potential CO_2 or brine migrations above the confining layer	Fluid sampling
CO_2 accumulations identified in the ACZ intervals	Pulsed neutron logging Time-lapse surface seismic data

Table 2-8: Observed changes in monitoring data that may trigger an AoR re-evaluation.

If the re-evaluated AoR is substantially different from the previous AoR, the project will identify all active and abandoned wells that penetrate the confining zone in the re-evaluated AoR and will perform corrective actions on those wells (40 CFR 146.84 (e)). As needed, all other plans, such as the Emergency and Remedial Response Plan, will be revised to account for the re-evaluated AoR and will submit those plans to the UIC Director for review and approval (40 CFR 146.84 (f)).

Note that seismic events are covered under the Emergency and Remedial Response Plan. A tiered approach to responding to seismic events will be based on magnitude and location. A notification procedure is provided in that plan.

2.6 References

Atherton, E., 1971, Tectonic development of the Eastern Interior Region of the United States: Illinois State Geological Survey Illinois Petroleum 96, p. 29-43.

Birkholzer JT, Nicot JP, Oldenburg CM, Zhou Q, Kraemer S, Bandilla K. Brine flow up a well caused by pressure perturbation from geologic carbon sequestration: Static and dynamic evaluations. International journal of greenhouse gas control 2011;5(4):850-61.

Burger C, Wortman D, Brown C, Hassan S, Humphreys K, Willford M. FutureGen 2.0 Pipeline and Regional Carbon Capture Storage Project-Final Report. Futuregen Industrial Alliance, Inc., Washington, DC (United States); 2016.

CMG-GEM. Advance compositional and GHG reservoir simulator user's guide. Calgary, Alberta 2016.

Cornet F. Results from the In-Situ Stress Characterization Program, Phase 1: Geomechanical Tests Conducted in the FutureGen Stratigraphic Well (FGA#1). The FutureGen Industrial Alliance, Inc. 2014.

DOE/EIS-0460. Final Environmental Impact Statement for the FutureGen 2.0 Project, Morgan County, Illinois. 2013.

Engelder T. Stress regimes in the lithosphere: Princeton University Press, 1992.
Enick RM, Klara SM. CO_2 solubility in water and brine under reservoir conditions. Chemical Engineering Communications 1990;90(1):23-33.

Fischietto NE. Lithofacies and Depositional Environments of the Cambrian Mount Simon Sandstone in the Northern Illinois Basin: Implications for CO_2 Sequestration (M.S. thesis, Purdue University); 2009.

Freiburg JT, Holland ME, Malone DH, Malone SJ. Detrital zircon geochronology of basal Cambrian strata in the deep Illinois Basin, USA: evidence for the Paleoproterozoic-Cambrian tectonic and sedimentary evolution of central Laurentia. The Journal of Geology. 2020 May 1;128(3):303-17.

Freiburg JT, Morse DG, Leetaru HE, Hoss RP, Yan Q. A Depositional and Diagenetic Characterization of the Mt. Simon Sandstone at the Illinois Basin - Decatur Project Carbon Capture and Storage Site, Decatur, Illinois, USA. Illinois State Geological Survey Circular 583. 2014

FutureGen Alliance, 2013, Underground Injection Control Permit Applications for FutureGen 2.0 Morgan County Class VI UIC Wells 1, 2, 3, and 4, FG-RPT-017.

Hall HN. Compressibility of reservoir rocks. Journal of Petroleum Technology 1953;5(01):17-9.

Jahediesfanjani H, Warwick PD, Anderson ST. 3D Pressure-limited approach to model and estimate CO_2 injection and storage capacity: saline Mount Simon Formation. Greenhouse Gases: Science and Technology 2017;7(6):1080-96.

Kestin J, Khalifa HE, Correia RJ. Tables of the dynamic and kinematic viscosity of aqueous NaCl solutions in the temperature range 20–150 C and the pressure range 0.1–35 MPa. Journal of physical and chemical reference data 1981;10(1):71-88.

Krevor SC, Pini R, Zuo L, Benson SM. Relative permeability and trapping of CO_2 and water in sandstone rocks at reservoir conditions. Water resources research 2012;48(2).

Kumar A, Noh M, Pope G, Sepehrnoori K, Bryant S, Lake L. Reservoir simulation of CO_2 storage in deep saline aquifers. SPE/DOE Symposium on Improved Oil Recovery: Society of Petroleum Engineers; 2004.

Land CS. Calculation of imbibition relative permeability for two-and three-phase flow from rock properties. Society of Petroleum Engineers Journal 1968;8(02):149-56.

Li YK, Nghiem LX. Phase equilibria of oil, gas and water/brine mixtures from a cubic equation of state and Henry's law. The Canadian Journal of Chemical Engineering 1986;64(3):486-96.

Lovell TR. An Intracratonic Record of North American Tectonics (Doctoral dissertation, Purdue University); 2017.

McCutcheon SC, Martin J, Barnwell T, Maidment D. Handbook of hydrology. Handbook of hydrology New York: McGraw-Hill 1993.

Mehnert E, Weberling PH. Groundwater Salinity within the Mt. Simon Sandstone in Illinois and Indiana. Illinois State Geological Survey, Prairie Research Institute.; 2014.

Nelson WJ. Structural features in Illinois. Illinois State Geological Survey, Bulletin no. 100. 1995.

Nghiem L, Sammon P, Grabenstetter J, Ohkuma H. Modeling CO_2 storage in aquifers with a fully-coupled geochemical EOS compositional simulator. SPE/DOE symposium on improved oil recovery: Society of Petroleum Engineers; 2004.

Nghiem L, Shrivastava V, Tran D, Kohse B, Hassam M, Yang C. Simulation of CO_2 storage in saline aquifers. SPE/EAGE Reservoir Characterization & Simulation Conference: European Association of Geoscientists & Engineers; 2009a. p. cp-170-00063.

Nghiem L, Shrivastava V, Tran D, Kohse B, Hassam M, Yang C. Simulation of CO_2 storage in saline aquifers. SPE/EAGE Reservoir Characterization & Simulation Conference2009b.

Nicot J-P, Oldenburg CM, Bryant SL, Hovorka SD. Pressure perturbations from geologic carbon sequestration: Area-of-review boundaries and borehole leakage driving forces. Energy Procedia 2009;1(1):47-54.

Palkovic MJ. Depositional characterization of the Eau Claire Formation at the Illinois Basin-Decatur Project: facies, mineralogy and geochemistry (M.S. thesis, University of Illinois at Urbana-Champaign); 2015.

Peng D-Y, Robinson DB. A new two-constant equation of state. Industrial & Engineering Chemistry Fundamentals 1976;15(1):59-64.

Raziperchikolaee S, Alvarado V, Yin S. Effect of hydraulic fracturing on long-term storage of CO_2 in stimulated saline aquifers. Applied energy 2013;102:1091-104.

Reesink AJ, Best J, Freiburg JT, Webb ND, Monson CC, Ritzi RW. Interpreting pre-vegetation landscape dynamics: The Cambrian Lower Mount Simon Sandstone, Illinois, USA. Journal of Sedimentary Research. 2020 Nov;90(11):1614-41.

Rowe Jr AM, Chou JC. Pressure-volume-temperature-concentration relation of aqueous sodium chloride solutions. Journal of Chemical and Engineering Data 1970;15(1):61-6.

Roy P, Morris JP, Walsh SD, Iyer J, Carroll S. Effect of thermal stress on wellbore integrity during CO_2 injection. International Journal of Greenhouse Gas Control 2018;77:14-26.

United States Environmental Protection Agency. Geologic Sequestration of Carbon Dioxide: Underground Injection Control (UIC) Program Class VI Well Area of Review Evaluation and Corrective Action Guidance. 2013: 96 p.

Willman, H.B., Atherton, E., Buschbach, T.C., Collinson, C., Frye, J.C., Hopkins, M.E. Lineback, J.A. and Simon, J.A. 1975. Handbook of Illinois Stratigraphy. Champaign, Illinois: Illinois State Geological Survey, Bulletin 95.